Universidade de Aveiro
Departamento de Eletrónica, Telecomunicações e Informática
2014

Bruno Miguel Fernandes Silva

Implementação de pré-codificador SM-MIMO para 4G/LTE em plataforma SDR

Implementation of a SM-MIMO precoder for 4G/LTE in a SDR platform

Universidade de Aveiro
Departamento de Eletrónica, Telecomunicações e Informática
2014

Bruno Miguel Fernandes Silva

Implementação de pré-codificador SM-MIMO para 4G/LTE em plataforma SDR

Implementation of a SM-MIMO precoder for 4G/LTE in a SDR platform

"*A gentleman who rode along the sidewalk in front of them, suddenly stepped off the conveyor belt, pulled a phone from his coat pocket, spoke a number into it and shouted: "Gertrude, listen, I'll be an hour late for lunch because I want to go to the laboratory. Goodbye, sweetheart!" Then he put his pocket phone away again, stepped back on the conveyor belt, started reading a book...*"

— Der 35. Mai oder Konrad reitet in die Südsee
Erich Kästner - 1931

Universidade de Aveiro
2014

Departamento de Eletrónica,
Telecomunicações e Informática

Bruno Miguel Fernandes Silva

Implementação de pré-codificador SM-MIMO para 4G/LTE em plataforma SDR

Implementation of a SM-MIMO precoder for 4G/LTE in a SDR platform

Dissertação apresentada à Universidade de Aveiro para cumprimento dos requisitos necessários à obtenção do grau de Mestre em Engenharia Eletrónica e Telecomunicações, realizada sob a orientação científica do Doutor Manuel Alberto Reis de Oliveira Violas, Professor auxiliar do Departamento de Eletrónica, Telecomunicações e Informática da Universidade de Aveiro, e do Doutor Adão Paulo Soares da Silva, Professor auxiliar do Departamento de Eletrónica, Telecomunicações e Informática da Universidade de Aveiro.

Dedico este trabalho à minha família, amigos e colegas.

o júri / the jury

presidente / president

Prof. Doutor Paulo Miguel Nepomuceno Pereira Monteiro
Professor Associado do Departamento de Engenharia Eletrónica, Telecomunicações e Informática da Universidade de Aveiro

vogais / examiners committee

Doutor Nelson José Valente Silva
Investigador, Pt Inovação e Sistemas

Professor Doutor Manuel Alberto Reis de Oliveira Violas
Professor Auxiliar do Departamento de Engenharia Eletrónica, Telecomunicações e Informática da Universidade de Aveiro

agradecimentos /
acknowledgements

Agradeço aos meus orientadores por toda a ajuda e apoio neste último ano. À minha família por todo o apoio e motivação ao longo do meu percurso académico. Agradeço aos colegas e amigos por toda a ajuda e apoio durante o meu percurso académico.

Palavras Chave

4G, LTE, SDR, OFDM, LTE, SM-MIMO, Multiplexagem espacial, Equalização, ZF, MMSE, Pré-Codificação, FPGA, System Generator, MIMO

Resumo

O tema central deste trabalho de dissertação centra-se no desenvolvimento e teste de novas técnicas para utilização em comunicações sem-fios de nova geração. Foca-se no uso de várias antenas, técnicas de pré-codificação e no uso de multiplexagem espacial em detrimento de diversidade, de forma a aumentar a largura de banda. Ao longo do documento são apresentadas várias técnicas de multiplexagem, bem como bases teóricas de propagação de sinais rádio e técnicas baseadas no uso de várias antenas no emissor e recetor (MIMO). Foi proposto um sistema de pré-codificação baseado em diversidade espacial. A implementação e teste do bloco pré-codificador SM-MIMO foi realizada em primeiro lugar usando um simulador Matlab para efeito de comparação. Foram implementados dois equalizadores: *Zero Forcing* (ZF) e *Minimum Mean Square Error* (MMSE); posteriormente procedeu-se à implementação em System Generator de um pré-codificador com equalização ZF, de forma a ser possível a sua implementação em FPGAs. Esta implementação foi igualmente validada por comparação com o bloco implementado em Matlab.

Keywords 4G, LTE, SDR, OFDM, LTE, SM-MIMO,Spatial Multiplexing,Precoding, ZF, MMSE, FPGA, System Generator, MIMO

Abstract

The main goal of this dissertation is the development and evaluation of new techniques to be used in new generation of wireless comunication devices. It focuses on the usage of multiple antennas (MIMO), precoding and the usage of spatial multiplexing in disregard of diversity techniques. This makes possible to increase data rates considerably. Throughout the document, are shown several multiplexing techniques, theoretical information about wireless propagation, and multiple antennas techniques. It was proposed and implemented a spatial multiplexing system. Firstly it was implemented in Matlab, with two precoders tested: Zero Forcing (ZF) and Minimum Mean Square Error (MMSE). Subsequently a System Generator implementation (this time with only ZF equalizer) was made in order to make possible the migration to FPGAs. Both implementations were tested and validated, we also concluded that ZF based pre-coder had a lower Bit Error Rate for the same Signal to Noise Ratio (SNR).

Contents

List of Figures

List of Tables

Glossary

1G First Generation. 1

2G Second Generation. 2

3G Third Generation. 2

3GPP Third Generation Partnership Project. i, iii, 1

4G Fourth Generation. i, 1, 2

5G Fifth Generation. 2

ADSL Asymmetric Digital Subscriber Line. 2

AGC Automatic Gain Control. 21

AMPS Advanced Mobile Phone System. 2

ARIB The Association of Radio Industries and Businesses, Japan. 1

ATIS The Alliance for Telecommunications Industry Solutions, USA. 1

AWGN Additive White Gaussian Noise. iii, 15, 16, 28

BER Bit Error Rate. iv, 12, 15, 16, 19, 28, 29, 37

BS Base Station. 3, 5, 14, 37

CCSA China Communications Standards Association. 1

CDMA Code Division Multiple Access. viii, 2

CLB Configurable Logic Block. iv, 23

CSI Channel State Information. 18, 19, 21

DFT Discrete Fourier Transform. 11

EDA Electronic Design Automation. 24

EEPROM Electrically-Erasable Programmable Read-Only Memory. 24

EGC Equal Gain Combining. 18

ETSI The European Telecommunications Standards Institute. 1

EV-DO Evolution-Data Optimized. 2

FDD Frequency Division Duplexing. 14, 18

FDM Frequency-Division Multiplexing. i, iii, v, 4, 9

FFT Fast Fourier Transform. 11

FPGA Field Programmable Gate Array. ii, v, 3, 4, 23–25, 27, 29, 37

GPRS General Packet Radio Service. 2

GSM Global System for Mobile Communications. 2

GUI Graphical User Interface. 25, 29

HDL Hardware Description Language. 23

HSDPA High-Speed Downlink Packet Access. 2

HSPA High Speed Packet Access. 2

HSUPA High-Speed Uplink Packet Access. 2

IDFT Inverse Discrete Fourier Transform. 11

IFFT Inverse Fast Fourier Transform. 11, 12

IP Internet Protocol. viii, 2

ISI Intersymbol interference. 10

JTAG Join Test Action Group. 24

LOG Logarithm base 10. vii

LOS Line-of-Sight. 5–7

LTE Long Term Evolution. i, 1, 2, 18

MIMO Multi-Input-Multi-Output. ii, iii, viii, 3, 14, 16, 17, 19, 21, 27

MISO Multiple Input Single Output. iii, 3, 16–18

MMSE Minimum Mean Square Error. iii, iv, 20, 21, 28, 29, 37

MRC Maximum-Ratio Combining. 17

MS Mobile Station. 5, 14, 37

NMT Nordic Mobile Telephone. 2

NTT Nippon Telegraph & Telephone Corp. 1, 2

OFDM Orthogonal Frequency Division Multiplexing. i, iii, 3, 4, 9–12, 28

OTP One-Time Programmable. 23

PSD Power Spectral Density. 8, 15

QoS Quality of Service. 2

RAM Random-Access Memory. 23

RF Radio Frequency. 3, 14

SC Selection Combining. 18

SDR Software Defined Radio. 3

SIMO Single Input Multiple Output. iii, 16, 17

SINR Signal-to-Interference-plus-Noise Ratio. 20

SISO Single Input Single Output. iii, 15, 17

SM-MIMO Spatial Multiplexing MIMO. ii, iv, 3, 19, 21, 27–35, 37, 39

SMS Short Message Service. 2

SNR Signal-to-Noise Ratio. iii, 15, 16, 18, 20, 28, 29

SRAM Static Random-Access Memory. 23

TDD Time Division Duplexing. 14, 18

TDM Time-Division Multiplexing. i, iii, v, 4, 8, 9

TDMA Time Division Multiple Access. 2

TTA Telecommunications Technology Association, Korea. 1

TTC Telecommunication Technology Committee, Japan. 1

UHF Ultra High Frequency. 5

UMTS Universal Mobile Telecommunications System. 2

USB Universal Serial Bus. 2

VHDL VHSIC Hardware Description Language. 23

VHF Very High Frequency. 5

VHSIC Very-High-Speed Integrated Circuits. viii

VoIP Voice Over IP. 2

WCDMA Wideband CDMA. 2

WiMAX Worldwide Interoperability for Microwave Access. 2

ZF Zero Forcing. iii, iv, 19–21, 28, 37

CHAPTER 1

Introduction

This chapter will present the mobile communications generations, motivations, objectives and outline the document structure.

1.1 4G/LTE by Third Generation Partnership Project (3GPP)

The development of Telecommunications in the last decades, made the communication between to persons in any two points of the earth surface, extending even into space. Remote locations became less common and concepts as: mobility, portability, mobile phone became part of our life. The main reasons for these outcomes were the low price and worldwide availability of telecommunication technology.

The globalization of telecommunications was only possible due to the efforts and work of the 3GPP [1] organization. 3GPP is a global standards-developing organization [2] comprised by six international standard's organizations [3]: The Association of Radio Industries and Businesses, Japan (ARIB), The Alliance for Telecommunications Industry Solutions, USA (ATIS), China Communications Standards Association (CCSA), The European Telecommunications Standards Institute (ETSI), Telecommunications Technology Association, Korea (TTA) and Telecommunication Technology Committee, Japan (TTC). This partnership gave birth to most of the telecomunications' wireless standards that we have today.

The Mobile communications technologies are usually categorized into generations. Each generation is characterized by an disruptive improvement in telecommunications' techniques. Until now, a new generation has been released approximately every 10 years (as shown in Figure 1.1).

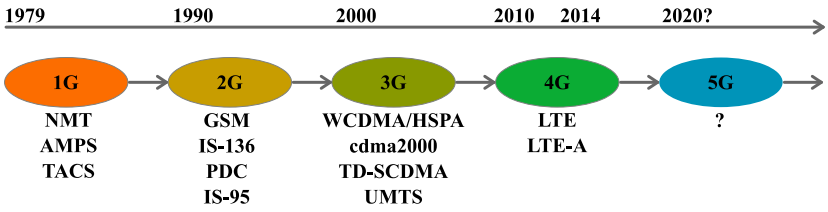

Figure 1.1: 3GPP Mobile Communication Generations

Those generations are categorized into [4]:

- The First Generation (1G) was characterized by being the generation of analogue cellular networks. The fist automatic, analogue cellular systems started working on the 1980s. Being first system introduced in Tokyo by Nippon Telegraph & Telephone Corp (NTT) on 1979 and

then widely deployed through the rest of Japan. Afterwards, another system was adopted in the Nordic countries by Nordic Mobile Telephone (NMT) (1981)and lastly the Advanced Mobile Phone System (AMPS) (1983). Over the following years other analogue systems were adopted throughout the rest of the world.

- The Second Generation (2G) was a great improvement of mobile communications, and marks the start of the digital cellular networks. The integration started around the 1990s with two major systems appearing on the market: the European Global System for Mobile Communications (GSM), Time Division Multiple Access (TDMA) based standard and the American, Code Division Multiple Access (CDMA) based. The two standards competed globally for the market supremacy. This phase was also characterized by the appearance of the prepaid mobile phones. The main highlights of this era: in 1991, the first GSM network on Finland was launched, in 1993 was introduced the world first smartphone (IBM Simon Personal Communicator) was introduced, the first Short Message Service (SMS) was sent on 3rd December 1992 between two machines and the Japanese company NTT introduced the first internet service in 1999. Following the standards "war", the first data systems implemented were CDMA2000 1X (CDMA based) and General Packet Radio Service (GPRS) (GSM based).
- Third Generation (3G) was introduced to cater the huge demand for data communications (Internet, and other broadband data). The main differences to the 2G was the data transmission which became packet switching based rather than circuit switching. Another difference was the imposition of a minimum data rate for indoors and outdoors. To archive those requirements, several technologies were developed. Once more, two rival standards appeared Wideband CDMA (WCDMA) (Universal Mobile Telecommunications System (UMTS)) and Evolution-Data Optimized (EV-DO). There were some new features introduced in the protocol in order to provide Voice Over IP (VoIP) such as Quality of Service (QoS) and real-time mechanisms. In mid 2000, in order to increase the data rate even further, the High Speed Packet Access (HSPA) family was implemented. High-Speed Downlink Packet Access (HSDPA) and High-Speed Uplink Packet Access (HSUPA), offering speeds of 14.4 Mbit/s for downlink and 5.76 MBit/s for uplink.
- The Fourth Generation (4G) is the current state of the art in public mobile communications. All the circuit switching were removed becoming full Internet Protocol (IP) networks. Two standards appeared, the Worldwide Interoperability for Microwave Access (WiMAX) and the Long Term Evolution (LTE). The technological improvement in this generation is to bring mobile ultra-broadband Internet access to laptops, smartphones, Universal Serial Bus (USB) dongles, and other devices.
- Fifth Generation (5G) is currently under development. There are three possible areas of improvement in comparison to the 4G namely: a super-efficient mobile network, super-fast mobile network and converged fiber-wireless networks.

1.2 MOTIVATION

In the last decades, there was an explosion in the usage of mobile phones, internet and other communications' services (as shown in Figure 1.2). The world population has migrated from fixed communications like telephones, payphones, Asymmetric Digital Subscriber Line (ADSL) and other fixed (wired)-broadband to a more portable/mobile scenario such as mobile/cellular telephones and mobile broadband.

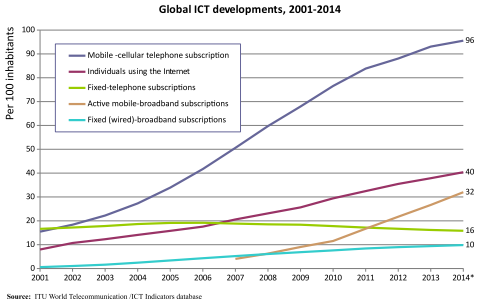

Figure 1.2: Evolution of various services subscriptions over time [5]

The rapid increase in cellular phones (see Figure 1.3a) and mobile broadband subscriptions (see Figure 1.3b) happens worldwide with developed countries having a more integration density than developing countries, but this demand for mobile communications becomes a worldwide problem. There is the need to implement more efficient and faster mobile communications to fulfil this wireless communications' demand. Telecommunications' engineers have the engagement to develop and improve the algorithms, Base Station (BS) cooperation, antennas, other Radio Frequency (RF) hardware's, improve efficiency as well as other technological improvements. This is an area of rapid growth and massive integration, so, even the smallest improvement translates into wealth and client satisfaction.

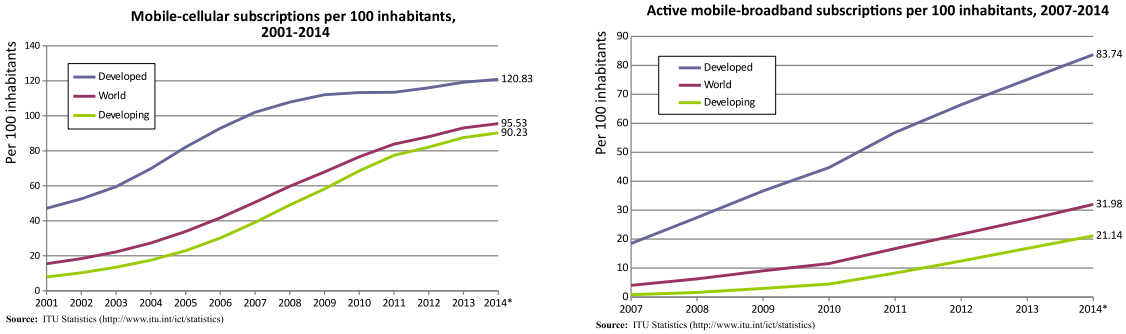

(a) (b)

Figure 1.3: Comparison between developed and underdeveloped countries [5]: (a) Mobile phone's subscriptions (b) Mobile-broadband subscriptions

1.3 OBJECTIVES

The main objective of this dissertation, is the implementation of an Software Defined Radio (SDR) based MIMO codification system, using FPGAs, and evaluate it's performance. Specifically, it is suggested that the implementation should be based upon, a previously implemented OFDM/Alamouti coding reference's chain, with MISO antennas setup. The chain should be extended to a MIMO [2x2] antenna setup. In order to achieve this extension, spatial multiplexing MIMO codification (SM-MIMO) is used, and an appropriate precoder/equalizer is implemented.

1.4 DOCUMENT STRUCTURE

This document is organized into six chapters as follows:

- Chapter 1 Introduction: at this chapter we can find the enumeration of the all mobile communications generations, as well as motivation, objectives and the document structure.
- Chapter 2 Wireless Signals Propagation: we start with a description of what is a wireless channel and propagation characteristics such as path loss, shadowing effect and multipath fading. Next we proceed with some multiplexing techniques (TDM, FDM and OFDM). The last section of this chapter talks about channel estimation and how can we invert its effects.
- Chapter 3 Multiple Antennas techniques: chapter at which, we discuss several diversity techniques (antennas, receive, and transmitter diversity), followed by the presentation of multiplexing techniques: spatial multiplexing and linear detection with and without precoding.
- Chapter 4 FPGAs: at this chapter we talk about FPGAs: what they are, how can we use them, and the Xilinx tool: System Generator.
- Chapter 5 Implementation and Results: this chapter presents the implementation of the proposed system and discusses the obtained results.
- Chapter 6 Conclusions and future work: this chapter presents the conclusions of this work and outlines some possible future work directions.

CHAPTER 2

WIRELESS SIGNALS PROPAGATION

This chapter presents the theoretical fundamentals and the state of the art in channel estimation and wireless propagation.

2.1 WIRELESS CHANNEL

Wireless channels, on the opposition to coaxial cables and other wired/waveguide's channels are, more dynamic and, most of the times, temporal and spatially dependent, that is, very unpredictable. The response of a wireless channel varies with the frequency, surroundings (buildings, vegetation,etc.), distance and orientation between Base Station (BS) and Mobile Station (MS), weather factors, existence of Line-of-Sight (LOS), interference of other sources, and many other parameters. On Very High Frequency (VHF) and Ultra High Frequency (UHF) bands, the propagation interference mechanisms such as diffraction, reflection, scattering, shadowing effect, etc. are more dominant.

Diffraction happen when the wireless signal is obstructed by surfaces with irregularities, creating secondary signals on the obstructing object and causing the original signal to change direction as shown in Figure 2.1a. Reflections on the other hand, occurs when radio wave collide with an object whose dimensions are larger than the radio wavelength (e.g. buildings) causing the wave to reflect on the obstacle's surface as shown in Figure 2.1b.

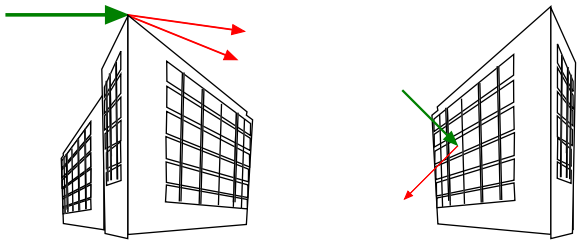

(a) (b)

Figure 2.1: Types of interference: (a) Diffraction and (b) Reflection

Other examples of waves' interferences are: Scattering, which happens when a signal wave propagates over a medium containing objects hich are smaller than the signal wavelength, as shown in Figure 2.2a and shadowing, witch this effect happens when there is an object, opaque to the signal radio waves, obscuring the MS as shown in Figure 2.2b.

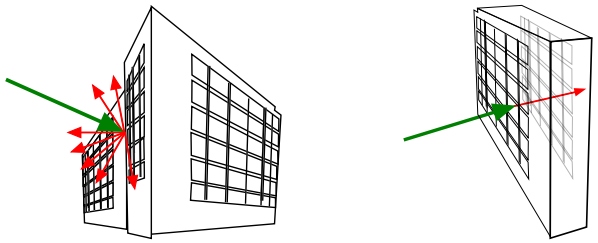

(a) (b)

Figure 2.2: Types of interference: (a) Scattering and (b) Shadowing

All of this signals' interferences can be categorized into three attenuations' categories:

1. Path Loss - Produces very slow attenuations over the distance as shown in Figure 2.3 and results from the reflections, scattering and free-space propagation attenuation.
2. Shadowing Effect - Results in slow fluctuations around a mean value.
3. Multipath fading - Induces fast attenuation variations resulting from the multiple reflections, scattering and diffractions in the surroundings.

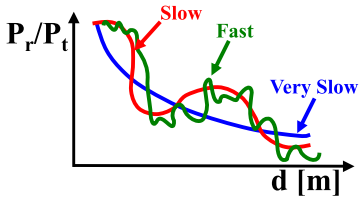

Figure 2.3: Different types of attenuations

2.1.1 PROPAGATION CHARACTERISTICS: PATH LOSS

As described in the previous section attenuation can happen in most distinct ways. To properly estimate/modulate mathematically the attenuation of a channel we should consider all the physics phenomenons. First of all lets take into account the attenuation in free space with Line-of-Sight (LOS). The first approach is to consider the attenuation of an isotropic antenna (Figure 2.4a).

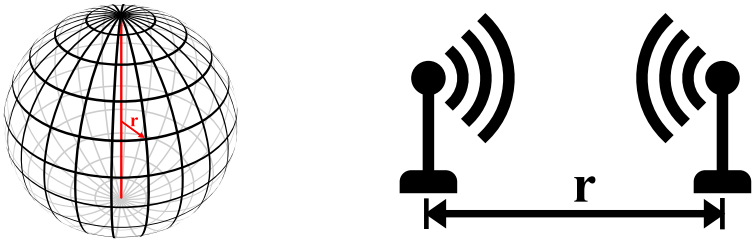

(a) (b)

Figure 2.4: Types of Antennas: (a) Isotropic (b) Directional

The power density of an isotropic antenna (Figure 2.4a) fed with power P_t at a r distance, is given by:

$$S_r = \frac{P_t}{4\pi r^2} \tag{2.1}$$

Assuming a lossless antenna at the receiver with an effective area of A_{eff}, the antenna receives the following power[6][7]:

$$P_r = A_{eff}\frac{P_t}{4\pi r^2} = \frac{P_t G_r \lambda^2}{(4\pi)^2 r^2} \tag{2.2}$$

Between two directional antennas (Figure 2.4b), the Friss formula is applied:

$$P_r = P_t\frac{G_r G_t \lambda^2}{(4\pi)^2 r^2} \tag{2.3}$$

From the Friis formula(Equation 2.3), we conclude that the signal attenuation depends mostly from the distance between antennas, and signal frequency. Other more realistic models exist, that consider for instance a ground reflection but even that model is only useful in LOS or quasi-LOS scenarios and other particularly simple scenarios.

When we stop having an LOS, other phenomenons start to show such as reflections, refractions, scattering, etc. as described in Section 2.1. We have to introduce these effects on the attenuation's modulation. Classical models do not cover all these effects, so empirical models started to appear. The most common simplified model considers the attenuation proportional to the power of the distance(r), that varies exponentially with the scenario considered [7].

$$P_r = P_t K \left[\frac{d_0}{d}\right]^{\gamma}, 2 \leq \gamma \leq 8 \tag{2.4}$$

Some common value sets for attenuation exponent (γ) are indicate in the Table 2.1.

Environment	**Attenuation exponent** (γ)
Free Space	2
Urban area cellular radio	2,7 to 3,5
Shadowed urban cellular radio	3 to 5
In building Line-of-Sight	1,6 to 1,8
Obstructed in buildings	4 to 6
Obstructed in factories	2 to 3

Table 2.1: Attenuation scenarios (source: [7])

Modern cellular communications are planned taking into account several empirical models, based on Equation 2.4.The most commonly used models in commercial planning systems are:

- Okumura model[8]
  - Empirical (requires knowledge about sites/frequency)
  - Not much practical (uses plots)
- Okumura-Hata Model[9]
  - Analytical approximation of Okumura model
- COST-136 Model
  - Extends Hata model for higher frequencies(2 GHz)
- Walfish/Bertoni (COST-231)
  - Extension of the COST-136 to include roof diffraction

2.1.2 SHADOWING EFFECT

This effect is modulated using a log-normal distribution, that is, it modules a fluctuation around a mean value. This behaviour can be explained using the law of large numbers. The power follows a Gaussian distribution with average $\mu = 0$ and a standard deviation range of $4 < \sigma < 12$ (empirical values). The received power is given by:

$$\mathrm{P_r} = \mathrm{P_t K} \left[\frac{\mathrm{d_0}}{\mathrm{d}}\right]^{\gamma} \psi, \quad \psi \text{ lognormal} \tag{2.5}$$

Or in logarithmic form[6][7]:

$$\frac{\mathrm{P_r}}{\mathrm{P_t}}\,(\mathrm{dB}) = 10 \log K - 10\gamma \log\left(\frac{\mathrm{d_0}}{\mathrm{d}}\right) + \psi_{\mathrm{dB}}, \quad \psi_{\mathrm{dB}} \sim \mathcal{N}\left(0, \sigma_{\psi}^2\right) \tag{2.6}$$

2.1.3 MULTIPATH FADING

Modeling the multipath reflections, diffractions and scattering effect is hard due to it's fast fluctuations and time dependency. Mathematical models are based on statistical analysis, considering random variables like: amplitude, phase, Doppler shift and time delay, resulting in a receiver signal constituted by the sum of all the different path signals added with the Doppler effect in the case where the receiver is moving, as shown in Equation 2.7.

$$\mathrm{r\,(t)} = \mathrm{Re}\left[\sum_{n=0}^{\mathrm{L(t)}} \alpha_{\mathrm{n}}\,(\mathrm{t})\,\mathrm{u}\,(\mathrm{t} - \tau_{\mathrm{n}}\,(\mathrm{t}))\, e^{\mathrm{j}(2\pi(\mathrm{f_o}+\mathrm{f_{D,n}(t)})(\mathrm{t}-\tau_{\mathrm{n}}(\mathrm{t})))}\right] \tag{2.7}$$

2.2 MULTIPLEXING TECHNIQUES

Most of the multiplexing mechanisms share the same goal: necessity to transmitting more than one type of message over the same channel. This can be achieved by dividing the channel into orthogonal slots. The most frequent types of slots are: time, frequency and a mixed (code division).

2.2.1 TIME-DIVISION MULTIPLEXING (TDM)

In time division multiplexing, slots are organized using sequential time periods. The Power Spectral Density (PSD) levels are time dependent, depending on the variation of amplitude of the signal. The TDM implementation requires a commutator at the transmitter, a distributor at the receiver end, and synchronization between the two devices[10].

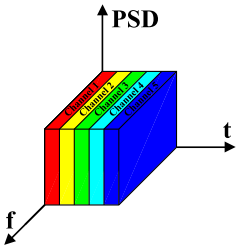

Figure 2.5: Time-Division Multiplexing (TDM)

2.2.2 Frequency-Division Multiplexing (FDM)

Frequency multiplexing as opposed to TDM, uses frequency slots to distinguish each channel. FDM implementations require modulator, filters and demodulators in order to alter the information at each frequency. FDM's filters play an important role in the multiplexing mechanism because, if the attenuation band of the filter isn't sharp enough, crosstalk will happen. Crosstalk means interference from adjacent channels, resulting in a corruption of the channel's data[10].

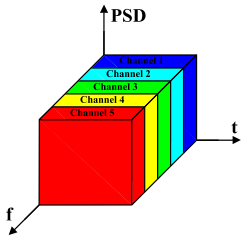

Figure 2.6: Frequency-Division Multiplexing (FDM)

In Table 2.2 we sumarize the main differences between TDM and FDM:

TDM	**FDM**
It is a technique for transmitting several messages on one channel by using independent time domain slots.	In this technique for transmitting several messages on one channel, by using independent frequency spectrum slots.
It requires commutator at the transmitting end and a distributor, working in perfect synchronization with the respective commutator at the receiving end.	Requires modulator, filters and demodulators.
Perfect synchronization between transmitter and receiver is required.	Synchronization between transmitter and receiver is not required.
Crosstalk problem is not severe	suffers from crosstalk problem due to imperfect bandpass filter.
It is usually preferred for digital signal transmission.	It is usually preferred for analogue signal transmission.
It does not require very complex circuitry.	It requires complex circuitry at transmitter and receiver.

Table 2.2: Comparison between TDM and FDM (source: [10])

2.2.3 Orthogonal Frequency Division Multiplexing (OFDM)

In order to increase the overall transmission bandwidth with low crosstalk and reduce the signal corruption resulting from radio-channel frequency selectivity, multi-carrier transmission is used. Multi-carrier work principle is based on the premise that instead of transmitting a single wideband signal, several narrowband signals are frequency multiplexed and transmitted jointly (those narrowband

signals are designated by sub-carriers). So at each instant (time), N sub-carriers are transmitted in parallel[2].

To increase the sub-carriers packaging (reduce the sub-carriers spacing), other signals formats where used as well as the orthogonal principle. The sinc and sinc-square-shaped frequency signals shown in Figure 2.7b suits those two principles. Although a sinc signal is overlapping there is still the possibility to archive orthogonality without Intersymbol interference (ISI), making it possible to transmit pulses (time domain of a sinc signal shown in Figure 2.7a) at a rate of 1/T with a bandwidth of $B = 1/(2T)$.

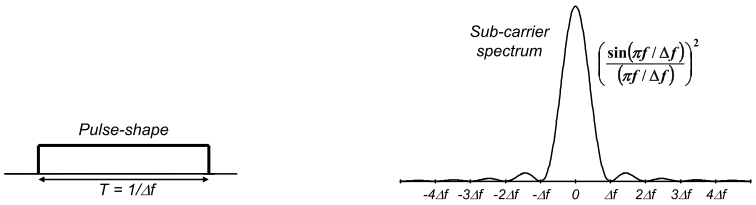

(a) (b)

Figure 2.7: Pulse signal single carrier: (a) Time domain (b) Frequency domain

In complex baseband notation, a basic OFDM signal x(t) during the time interval $mT \leq t < (m+1)T$ can be expressed as[2]:

$$x(t) = \sum_{k=0}^{N_c-1} x_k(t) = \sum_{k=0}^{N_c-1} a_k^{(m)} e^{j2\pi k\Delta f t} \tag{2.8}$$

where $x_k(t)$ is the k^{th} modulated sub-carrier having a frequency $f_k = k\Delta f$ and $a_k^{(m)}$ the modulation symbol applied to the k^{th} sub-carrier during the m^{th} OFDM symbol interval ($mT \leq t < (m+1)T$). In each OFDM symbol N modulated (example of modulations: BPSK, QPSK, QAM-16, QAM-64, etc.) symbols are transmitted in parallel (see Figure 2.8).

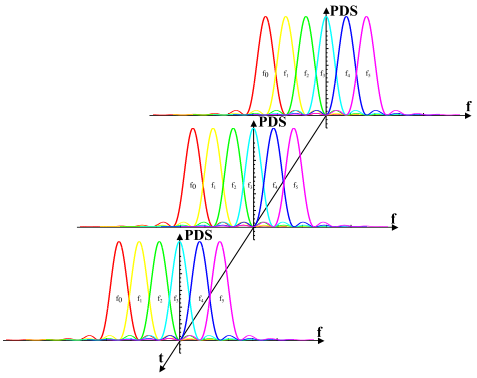

Figure 2.8: OFDM sub-carriers symbols

To prove the orthogonality between two sub-carriers we take into account two sub-carriers x_{k_1} and x_{k_2} over a time interval $mT \leq t < (m+1)T$, integrating the multiplication of one of the sub-carriers by the conjugate of the other one (over that time period), we get:

$$\int_{mT}^{(m+1)T} x_{k_1}(t)\, x_{k_2}^*(t)\, dt = \int_{mT}^{(m+1)T} x_{k_1} x_{k_2}^* e^{j2\pi k_1\Delta f t} e^{-j2\pi k_2\Delta f t}\, dt = 0 \qquad \text{for } k_1 \neq k_2 \tag{2.9}$$

proving that sub-carriers are indeed orthogonal. We can also define the modulations as a set of orthogonal functions $\varphi(t)$:

$$\varphi(t) = \begin{cases} e^{j2\pi k\Delta ft} & 0 \leq t < T \\ 0 & \text{otherwise} \end{cases} \tag{2.10}$$

OFDM modulation can be archived resorting to a bank of modulators as shown in Figure 2.9a, to perform the demodulation, a bank of correlators can be used, one for each sub-carrier shown in Figure 2.9b.

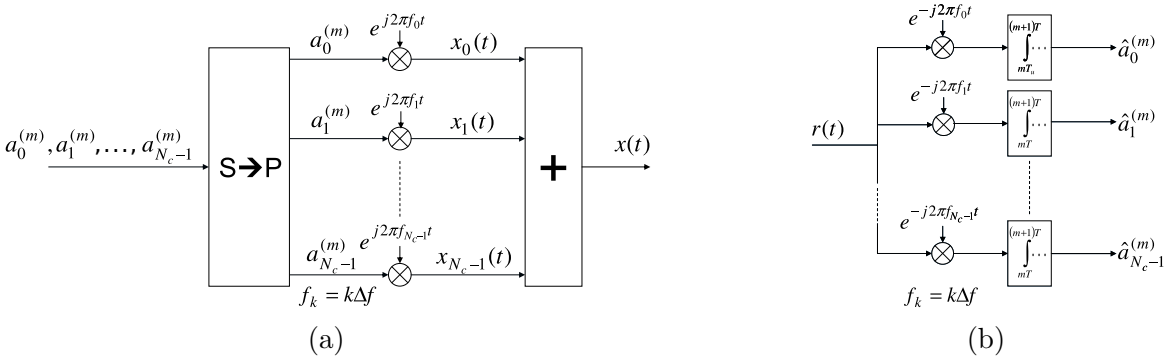

Figure 2.9: OFDM banks: (a) modulator (b) correlator/demodulator

But this implementation is not the most efficient and it requires a lot of hardware resources. The sub-carriers being orthogonal and having a constant bit rate separation of $1/T$ makes possible to implement a low-complexity and computationally efficient demodulator using Fast Fourier Transform (FFT) processing[2]. Having a sampling frequency of f_s multiple of the sub-carrier spacing $\Delta f = 1/T = N\ \Delta f$, N parameters should be chosen so that the sampling theorem[11] is satisfied. We can describe a time-discrete OFDM signal as:

$$x_n = x(nT_s) = \sum_{k=0}^{N_c-1} a_k e^{j2\pi k\Delta fnT_s} = \sum_{k=0}^{N_c-1} a_k e^{j2\pi kn/N} = \sum_{k=0}^{N-1} a'_k e^{j2\pi kn/N} \tag{2.11}$$

With a'_k equal to:

$$a'_k = \begin{cases} a_k & 0 \leq k < N_c \\ 0 & N_c \leq k < N \end{cases} \tag{2.12}$$

This means that the sequence x_n, the OFDM sampled signal is an N-size Inverse Discrete Fourier Transform (IDFT) and if we chose the IDFT size (N) equal to a power of two (2^m), we can perform the OFDM with a radix-2 Inverse Fast Fourier Transform (IFFT) processing. Regarding the demodulation, there is also an alternative to substitute the parallel correlators' bank with an efficient FFT processing or similarly to the modulator, a Discrete Fourier Transform (DFT) with size N.

In order to keep the orthogonality we must ensure that there aren't any frequency-domain corruption (frequency-selective radio channel for instance). In order to assure that, a band-guard is added: Cyclic-Prefix. This could be done in many different ways, for instance, putting zeros at the beginning of the symbol, but that would interfere with the demodulation process because that part of the ofdm symbol will not suffer the same interference as the rest of the symbol. Instead of that, a portion of the end $t = T_{CP}$ is copied to the start of the OFDM symbol. This increases the OFDM symbol size by T_{CP}.

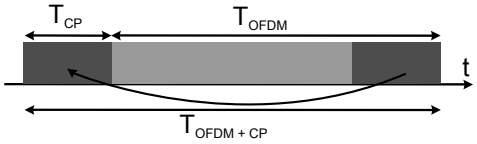

Figure 2.10: OFDM symbol with Cycle-Prefix

2.3 CHANNEL ESTIMATION

Typical OFDM systems generate data, modulates it, converts them to time domin using a IFFT block, and then sends the symbols over a (wireless) channel. But because how wireless signals propagate, those signals will be distorted as explained in Chapter 2.1.

Channel estimation is often performed to improve the communication between transmitter(s) and receiver(s). With channel information we can counterbalance the effects of the channel by, for instance, compensating the frequency selective fading, or even apply channel multiplexing techniques, improve BER, etc.

Several techniques can be used to estimate the channel response, and those processes can be performed at the transmitter side or in the receiver side.

2.3.1 RECEIVER SIDE

Recalling the OFDM system, an OFDM symbol is a sequence of orthogonal sub-carriers. Their orthogonality makes possible to approximate the received signal as a product of sub-carriers' components by the frequency response of the channel. This makes possible to identify the frequency response of the channel just by comparing a known signal transmitted with the received version of it[12] or also a known data sequence (eg: preamble or training sequences). These known (typically it is known the signal frequency, amplitude and phase) signals are designated pilots. One of the drawbacks of using pilots in some sub-carriers, is that the effective bandwidth decreases[13]. In order to keep the bandwidth as high as possible, instead of using pilots on every carriers, is commonly used a fixed amount of pilots and then interpolation is performed to find the other sub-carriers' channel response.

The arrangement of the pilots inside an OFDM symbol can be realised in three distinct ways: block, comb and lattice type[14]. In pilots' block type arrangement, depicted in Figure 2.11, the pilots are transmitted periodically (time domain) with a separation period of S_t. The channel estimation on the OFDM sub-carriers in-between is performed by interpolation. The S_t distance must satisfy the following channel coherence time [1] relation:

$$S_t \leq \frac{1}{f_{Doppler}} \tag{2.13}$$

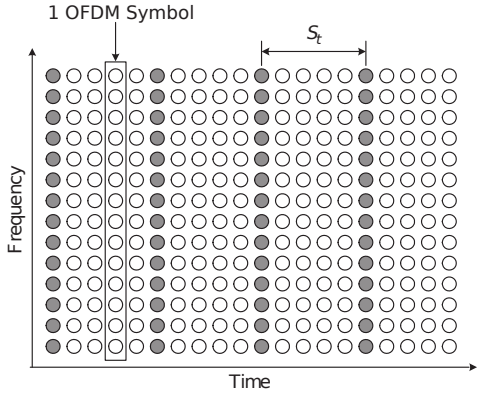

Figure 2.11: Pilots arrangement: Block-Type (adapted from: [14])

Other pilots frequency/time organization are possible, we will present two more possibilities as an example: comb-type and lattice.

[1]The coherent time T_c measures how fast the channel changes in time. It is defined as the time delay for which the signal autocorrelation coefficient reduces to 0.7. Usually the approximation $T_c \approx 1/f_{Doppler}$ is applied[15]

At Figure 2.12a we depict a Comb-type pilot arrangement, at this version the pilots are placed along fixed frequencies and for the rest of the sub-carriers a frequency interpolation is performed. Comb-type pilots arrangement have a good performance in fast-fading channels, on the opposition to the block-type which has better performance in frequency-selective channels (but not comb-type). Due to frequency-selective channel characteristics, pilots frequency spacing must be carefully selected so that matches channel coherent bandwidth[2] requirements. So S_f must satisfy the inequality[3]:

$$S_f \leq \frac{1}{2\pi\sigma_\tau} \approx \frac{1}{\sigma_\tau} \tag{2.14}$$

At Figure 2.12b we have a mixture of the two previous types, pilots are placed along frequency and time simultaneously, having a frequency spacing re-usage of S_f and S_t for time spacing separation [14]. The S_t and S_f must satisfy the channel time coherence and channel frequency coherence simultaneously, so it must satisfy the two previously presented relations:

$$S_t \leq \frac{1}{f_{Doppler}} \quad \wedge \quad S_f \leq \frac{1}{\sigma_\tau} \tag{2.15}$$

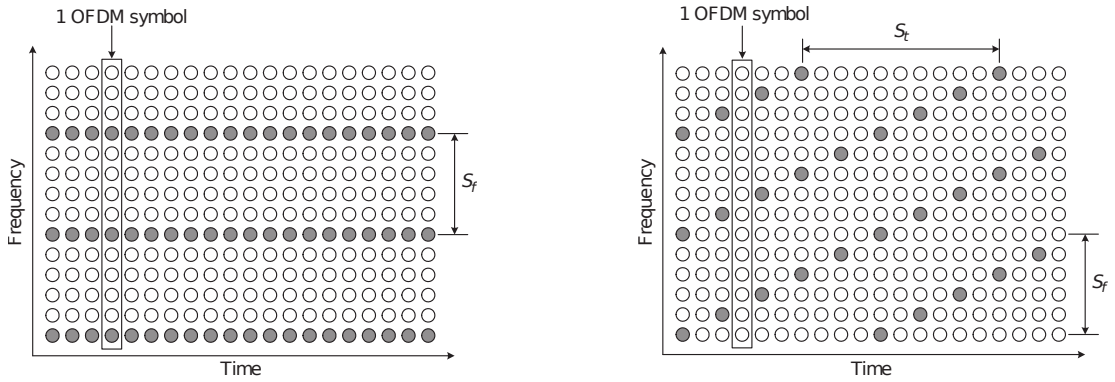

(a) (b)

Figure 2.12: Pilots arrangement: (a) Comb-type (b) Lattice-type (adapted from: [14])

Other receiver side's channel estimation techniques are presented by Y. S. Cho *et al.* [14] namely:

- Training Symbol-Based Channel Estimation.
- LS Channel Estimation.
- MMSE Channel Estimation.
- DFT-Based Channel Estimation
- Decision-Directed Channel Estimation
- Channel Estimation Using a Superimposed Signal
- Channel Estimation in Fast Time-Varying Channels
- EM Algorithm-Based Channel Estimation
- Blind Channel Estimation

[2]Channel coherence bandwidth B_c is considered to be the maximum frequency interval $(\Delta f)_{max}$ that limits the correlation coefficient ρ to be smaller than a given threshold, typically < 0.7 [15]

[3]σ_τ: delay spread

2.3.2 TRANSMITTER SIDE

In most circumstances, the transmitter (BS) doesn't have direct access to the channel on it side, since the channel is in "front" of it, so indirect techniques must be used. In Time Division Duplexing (TDD) multiplexing systems, channel reciprocity[4] is verified, so we can transmit from BS to MS and then estimate the channel on the uplink (from MS to BS). Regarding Frequency Division Duplexing (FDD) systems, the channel reciprocity[4] doesn't hold, so downlink channel information must be relayed back from MS to the BS.

CHANNEL RECIPROCITY

In order to use channel reciprocity, the channel gains in both directions, must be highly correlated (depicted in Figure 2.13, $H_{Tx,ij} \approx H_{Rx,ij}$), this can only be archived using a TDD scenario since all and the same frequencies are used in both direction. FDD systems, by using different frequencies for each direction, the reciprocity doesn't hold. Channels reciprocity discrepancies may appear in systems with reciprocal channels. Because Radio Frequency (RF) components in forward and backwards direction have a different response, RF characterization and compensation must be performed.

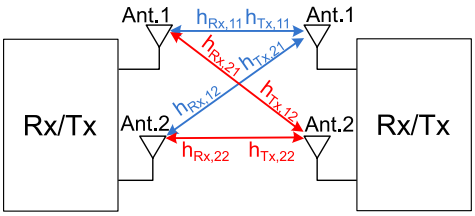

Figure 2.13: Reciprocal MIMO channel

RELAY CHANNEL

This method makes possible to determinate the channel parameters without the need to compensate the RF directional offset and other reciprocal interferences, also makes possible to determine channel parameters in FDD systems and other multiplexing techniques that makes the channel non reciprocal. In Figure 2.14 we can watch how the channel relay works: parameters are determined on the receiver and then sent back to the emitter using a uplink that may not be related to the downlink one. This means, $H_{Tx,ij} \neq H_{Rx,ij}$

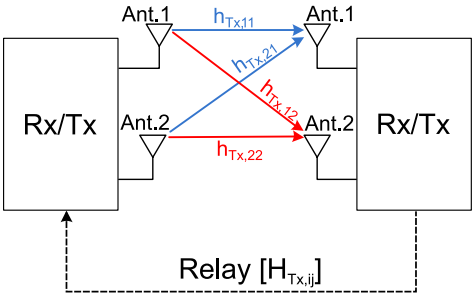

Figure 2.14: Relay MIMO channel

[4]Channel reciprocity means that the downlink and the uplink channels' parameters are approximately the same

CHAPTER 3

Multiple Antennas techniques

This chapter presents several multiple antennas techniques as well as equalization mechanisms.

When we talk about multiple antennas techniques, there are two major categories: diversity and multiplexing techniques. The differential aspect about these two is the tradeoff between improving Bit Error Rate (BER) or increasing data rate respectively.

As described in Section 2.1, wireless signals suffer from fading due to propagation effects, resulting into level, frequency and delay fluctuations, which have a negative influence on the system's performance. By using multiple antennas, additional degrees-of-freedom appear as well as: power, spatial and directional gain[2][16][17][14].

Lets first analyse the case of a SISO antenna setup shown in Figure 3.2a and the probability errors of it's channel for future comparison purposes. The signal received after passing through a AWGN channel is given by: $y(t) = s(t) + n(t)$, with $n(t) \rightarrow \mathcal{CN}(0,1)$: a white Gaussian random process with mean zero and PSD $N_0/2$. If the s(t) signal is modulated by: $s(t) = \mathcal{R}e\left\{u(t)e^{j2\pi f_c t}\right\}$, and if the bandwith of the complex envelope u(t) of s(t) is B, then the transmitted signal s(t) bandwidth is 2B. And since the noise has an uniform PSD of $N_0/2$, this means that in the 2B bandwith the noise power is $2B \times N_0/2 = N_0B$. The SNR[1] at the receiver is then[18]:

$$SNR = \frac{P_T}{N_0 B} = \frac{E_b}{N_0 B T_b} \tag{3.1}$$

with E_b the bit energy and T_b the bit period. Defining P_s the symbol error probability, then the bit error probability is:

$$P_b = \frac{P_s}{\log_2 M} \tag{3.2}$$

with M the M-aray signalling, meaning that the bit error probability varies with the signal modulation used.

Using a Rayleigh Flat Fading Channel, the receiver signal is then given by: $y = hs + n$ with $h \sim \mathcal{CN}(0,1)$, the fading coefficient. In this channel, the instantaneous SNR is given by:

$$SNR(h) = |h|^2 \overline{SNR} \tag{3.3}$$

with $\overline{SNR}$ the average SNR. The error probability in this case is:

$$P_e = \Psi\mathcal{Q}\left(\sqrt{|h|^2 \beta SNR_s}\right) \tag{3.4}$$

[1]SNR is the ratio of the received signal power P_r to the power of the noise within the bandwidth of the transmitted signal s(t)

$\mathcal{Q}$ is a Gaussian function. Depicting Figure 3.1 we verify that at AWGN channels the probability error decay more rapidly with the increase of SNR levels.

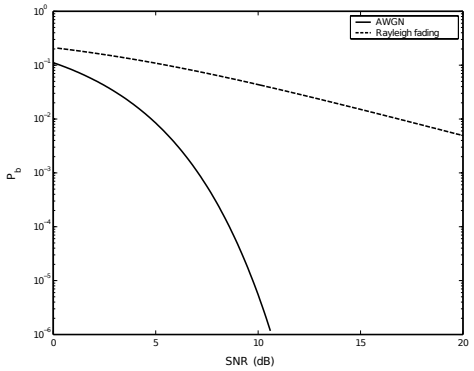

Figure 3.1: Error probability of AWGN and Rayleigh Flat Fading channels

3.1 DIVERSITY TECHNIQUES

Diversity techniques are based in the assumption that instead of having a single path, several other independent paths are created and with this method we expect to decrease BER. The amount of improvement in BER we can achieve depends on the current channel state. In Good states, the SNR is high enough to achieve reliability. On the other hand, bad states with a low SNR, reliability will not be accomplished. In Gaussian noise scenarios, the bad state of the channel will take a more important rule in error probability since the $\mathcal{Q}$ curve function is dominated by the behaviour of bad states. In the case of a Rayleight fading, the probability of a channel be bad is proportional to the inverse of SNR ($P_e \propto 1/SNR$), using L diversity paths then the probability error is:

$$P_e \propto \frac{1}{SNR^L} \tag{3.5}$$

this means that we can have the same probability error, using different levels of power, just by increasing the number of paths (this results in an increase of power efficiency). If we are more interested in improving the BER, then an increase in the number of paths, while maintaining the SNR value (or increasing it) does the job.

Other examples of diversity applicability are across time (eg: repeating the same information at different time slots), frequency (eg: transmitting the same signal at different carriers) and space (eg: sending the same information through different antennas), angular, polarization, macrodiversity, and cooperative diversity[15].

3.1.1 ANTENNAS DIVERSITY

With a sufficient inter-antenna distance or using different antennas polarizations, each channel will have a low mutual correlation and provides additional diversity against fading on the radio channel. A main advantage of using antennas diversity instead of using frequency, time or other diversity techniques, is that independent paths can be realized without the need to increase SNR, bandwidth or transmission delays. Antennas diversity can be achieved at the receiver or the transmitter depending on the antenna setup. SIMO antennas depicted in Figure 3.2b use receive diversity while MISO setup depicted in Figure 3.2c has transmit diversity. Both transmit and receive diversity can be achieved using MIMO antennas shown in Figure 3.2d. These two types of diversity will be presented in the next subsections: 3.1.2 and 3.1.3.

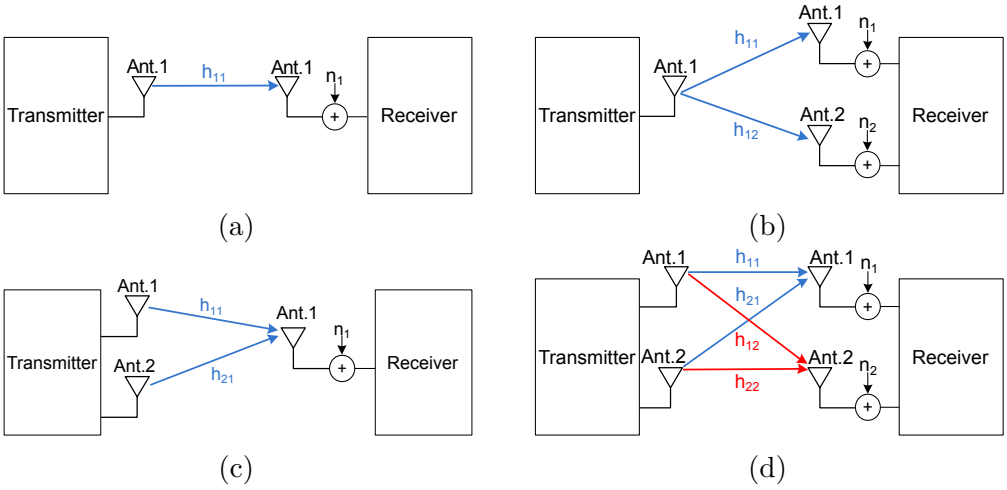

Figure 3.2: Antenna setups: (a) SISO (b) SIMO (c) MISO (d) MIMO

3.1.2 RECEIVE DIVERSITY

Receive diversity can be accomplished through the usage of diversity gain (the principle is that channels are independent) or antenna gain (the diversity is achieved based that the noise sources are independent for each receiver, see Figure 3.2b and 3.2d). In matrix notation, the y_i signals received at each antenna, for an $n \times m$ antenna setup (n antennas at the transmitter and m antennas at the receiver) is given by:

$$\begin{bmatrix} y_1 \\ y_2 \\ \vdots \\ y_m \end{bmatrix} = \begin{bmatrix} h_{1,1} & h_{1,2} & \cdots & h_{1,m} \\ h_{2,1} & h_{2,2} & \cdots & h_{2,m} \\ \vdots & \vdots & \ddots & \vdots \\ h_{n,1} & h_{n,2} & \cdots & h_{n,m} \end{bmatrix} \times \begin{bmatrix} s_1 \\ s_2 \\ \vdots \\ s_n \end{bmatrix} + \begin{bmatrix} n_1 \\ n_2 \\ \vdots \\ n_m \end{bmatrix} \Leftrightarrow Y = Hs + n \tag{3.6}$$

h_i are the complex channel gains, s_i are the signals transmitted at each emitter antenna and n_i are the noise terms captured at each receiver antenna.

If we linearly combine the y_i signals with weight signals: $g_1, g_2, g_3, \cdots, g_m$ (see Figure 3.3) we can archive diversity, as shown in Figure 3.3

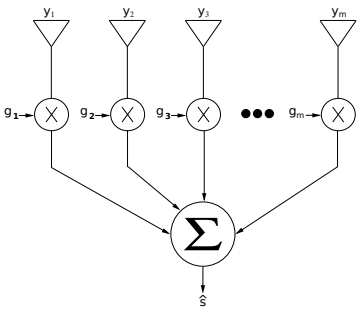

Figure 3.3: Linearly combine signals at the receiver

Depending on the weights chosen, the estimated data symbols ($\hat{s}$) will vary, as well as the error rate. Erik Dahlman *et al.* [2] presents several solutions: Maximum-Ratio Combining (MRC) $(g_i = h^*)^2$ that produces a phase rotation at the different antennas to compensate for corresponding channel

[2] * is the complex conjugate

phases' rotations and produces a gain correction in the proportion of the corresponding channel gains.

$$\hat{s} = \sum_{i=1}^{m} |\mathrm{h_i}|^2 \, \mathrm{s} + \sum_{i=1}^{m} \mathrm{h_i^*} \mathrm{n_i} \tag{3.7}$$

In Equal Gain Combining (EGC) the weights are given by: $\mathrm{g_i} = \mathrm{h}^*/|\mathrm{h}|$, this technique cophases signals on all receivers and combines them with equal gain resulting into a estimate symbol of:

$$\hat{s} = \sum_{i=1}^{m} |\mathrm{h_i}| \, \mathrm{s} + \sum_{i=1}^{m} \frac{\mathrm{h_i^*}}{|\mathrm{hi}|} \mathrm{n_i} \tag{3.8}$$

In Selection Combining (SC) diversity, the received signal with highest SNR is selected for decoding. This selection is made by comparing the instantaneous amplitude of each signal and choose the highest one. Performance analysis and comparison between these linear combining techniques are presented in [18] and [19]

3.1.3 TRANSMITTER DIVERSITY

Regarding the diversity techniques at the transmitter(applicable in MISO antenna setup for instance), they can be divided into two major types: open loop and closed loop techniques. When the diversity is applied at the transmitter, a common symbol will be sent in several antennas, pass through different channels and received in a common antenna[18] as shown in Figure 3.2c.

OPEN LOOP TECHNIQUES

In open loop techniques, Channel State Information (CSI) is not available at the transmitter side. Space-Time and frequency encoding are applicability examples of this technique. To make sure we can process the signals at the receiver, the symbols cannot be transmitted simultaneously in every emitter since the received signal would be:

$$\mathrm{y(t)} = \mathrm{sh_1} + \mathrm{sh_2} = \mathrm{s(h_1 + h_2)} \tag{3.9}$$

The received symbols have a dependency of the two channels simultaneously, to mitigate this space-time codes are needed. Space-time block codes are build from known orthogonal designs, they are easy to decode and is possible do achieve full diversity but contrarily to space-time trellis codes, they don't have coding gain. Space-time trellis codes on the other hand, are complex to decode [20].

The Alamouti coding [21] currently used in LTE is an example of orthogonal space-time block code (See Table 3.1 for the example for 2 transmitter antennas). Symbols are transmitted across space (using the two antennas) and time (using two transmission intervals), also $\mathrm{s_n^*}$ represents the complex conjugate of $\mathrm{s_n}$ [20].

time/frequency	**Antenna 1**	**Antenna 2**
n	$\mathrm{s_n}$	$-\mathrm{s_{n+1}^*}$
n + 1	$\mathrm{s_{n+1}}$	$\mathrm{s_n^*}$

Table 3.1: Alamouti coding

CLOSED LOOP TECHNIQUES

Contrarily to open loop, the closed loop technique requires the transmitter to know CSI. Two typical transmitter diversity closed loop based techniques are: precoding and beamforming [16]. Beamforming provides simultaneously decent diversity and a power gain, which is obtained through the coherent addition of user signals. Remembering the channel estimation techniques in Section 2.3, the same principle can be used here: CSI can be estimated at the transmitter (eg:TDD) or relayed (eg: FDD).

3.2 MULTIPLEXING TECHNIQUES

In the last section we introduced the diversity and how we can improve BER but if we are interested in achieving higher bit rates (also called channel capacity), multiple antennas multiplexing techniques are a better choice [16].

In order to increase data rate, some concessions have to be made. The knowledge of CSI at the transmitter and receiver, as well as using MIMO antennas, brings various degrees-of-freedom that can then be "exchanged" for data rate. A typical multiplexing mechanism that uses all these suppositions is the Spatial Multiplexing MIMO (SM-MIMO).

3.2.1 Spatial Multiplexing MIMO (SM-MIMO)

SM-MIMO is a MIMO technique that uses spatial multiplexing to create independent data streams. Comparatively with other MIMO systems, SM-MIMO can achieve higher data speeds acting as a 'data-rate-booster'[22]. Under certain conditions, with MIMO spatial multiplexing, we can make the rate increase almost linearly with the number of antennas, making it possible to increase the data rate virtually without saturation. Considering a [2x2] antenna setup (2 antennas at the transmitter and 2 at the receiver) then the signals at the receiver antennas are:

$$\begin{bmatrix} y_1 \\ y_2 \end{bmatrix} = \begin{bmatrix} h_{1,1} & h_{1,2} \\ h_{2,1} & h_{2,2} \end{bmatrix} \times \begin{bmatrix} s_1 \\ s_2 \end{bmatrix} + \begin{bmatrix} n_1 \\ n_2 \end{bmatrix} \Leftrightarrow y = Hs + n \tag{3.10}$$

Where H is a matrix of $h_{i,j}$ channels' complex coefficients, s is a vector of s_i transmitted symbols and n is a vector of n_i noise sources added at each receiver as shown in Figure 3.2d. Assuming there is no noise sources and the channel matrix H is invertible then we can perfectly recover the s symbols by multiplying the received vector y with a matrix $W = H^{-1}$ this is:

$$\begin{bmatrix} \hat{s}_1 \\ \hat{s}_2 \end{bmatrix} = Wy \Leftrightarrow \begin{bmatrix} \hat{s}_1 \\ \hat{s}_2 \end{bmatrix} = H^{-1}Hs + H^{-1}n \Leftrightarrow \begin{bmatrix} \hat{s}_1 \\ \hat{s}_2 \end{bmatrix} = s + H^{-1}n \tag{3.11}$$

Perfect recovery is only achieved in the case of a noiseless system. We can also corroborate that when the channel matrix becomes closer to singular, the noise level will increase[22]. This detection mechanism is called linear reception/demodulation of spatially multiplexed signals.

3.2.2 linear signal detection for SM-MIMO

Other more sophisticated linear signal detection mechanisms exist, next we will present some examples (see Figure 3.4 for a block-set of a linear detection mechanism for spatial multiplexing).

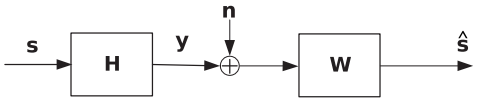

Figure 3.4: Linear signal detection at the receiver block-set

Zero Forcing (ZF) signal detection

The ZF detector nullifies the interference from adjacent signals using the following coding matrix W_{ZF}:

$$W_{ZF} = \begin{bmatrix} W_{00} & W_{01} \\ W_{10} & W_{11} \end{bmatrix} = H^H \left(HH^H \right)^{-1} \tag{3.12}$$

This operation reverses the channel effect by inverting the channel, when the matrix H is non square, a pseudoinverse operation should be performed thence the Equation:3.12. $(\cdot)^{\mathrm{H}}$ represents the Hermitian transpose operation. The solution of the pseudoinversion is the one and only one solution and coincides with the solution for the system $Hy = s$ if H is invertible[3] [23]. The received signals are then[14]:

$$\begin{aligned} \hat{\mathrm{s}} &= \mathrm{W}_{\mathrm{ZF}}\mathrm{y} \\ &= s + \mathrm{H}^{\mathrm{H}}\left(\mathrm{H}\mathrm{H}^{\mathrm{H}}\right)^{-1}\mathrm{n} \end{aligned} \tag{3.13}$$

If the antenna setup produces a rectangular channel matrix H, the channel inversion can be simplified to:

$$\mathrm{W}_{\mathrm{ZF}} = \begin{bmatrix} W_{00} & W_{01} \\ W_{10} & W_{11} \end{bmatrix} = \mathrm{H}^{-1} \tag{3.14}$$

Minimum Mean Square Error (MMSE) signal detection

The MMSE detector maximizes the post-detection Signal-to-Interference-plus-Noise Ratio (SINR), and it's matrix is given by:

$$\mathrm{W}_{\mathrm{MMSE}} = \begin{bmatrix} W_{00} & W_{01} \\ W_{10} & W_{11} \end{bmatrix} = \mathrm{H}^{\mathrm{H}}\left(\mathrm{H}\mathrm{H}^{\mathrm{H}} + \sigma_{\mathrm{z}}^2\mathrm{I}\right)^{-1} \tag{3.15}$$

note that for this linear detection to work, the statistical information of the noise σ_{z}^2 is necessary. Similarly to ZF, the received signals are:

$$\begin{aligned} \hat{\mathrm{s}} &= \mathrm{W}_{\mathrm{MMSE}}\mathrm{y} \\ &= s + \mathrm{H}^{\mathrm{H}}\left(\mathrm{H}\mathrm{H}^{\mathrm{H}} + \sigma_{\mathrm{z}}^2\mathrm{I}\right)^{-1}\mathrm{n} \end{aligned} \tag{3.16}$$

A performance evaluation of the equalizers at the receiver side was performed by Y. Jiang et. al. [24] (see Figure 3.5)

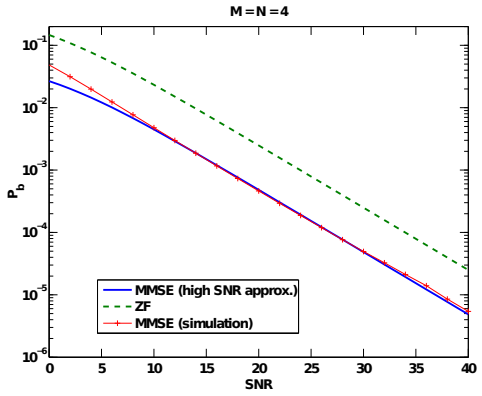

Figure 3.5: Error probabilities of ZF and MMSE (Monte Carlo trials and high SNR approximation) M=N=4 (source [24])

[3] A solution of a Pseudoinversion to be unique it's matrix H has the following proprieties:

- The columns of H are linearly independent.
- The nullspace of H contains only the zero vector.
- The rank of H is n.
- The square matrix $\mathrm{H}\mathrm{H}^{\mathrm{H}}$ is invertible.

3.2.3 Spatial Multiplexing MIMO (SM-MIMO) with precoding

If we have the CSI at the transmitter side we can linearly pre-equalize also known as precoding shown in Figure 3.6.

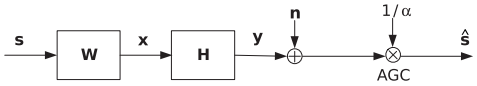

Figure 3.6: Linear pre-equalization block-set

Precoding is represented by the matrix W which is multiplied to the data symbols vector s, that is:

$$\mathrm{x} = \mathrm{W}\mathrm{s} \tag{3.17}$$

to determine the W precoding matrix ZF of MMSE linear equalizers can be used. It is also a good idea to constraint the total transmitted power so W is multiplied by α, note that to amend this amplification factor, at the receiver we have to divide the receiver signal by α (through Automatic Gain Control (AGC) or digitally):

$$\alpha_{\mathrm{eq}} = \sqrt{\frac{\mathrm{N_T}}{\mathrm{Trace}\left(\mathrm{W_{eq}} \cdot \mathrm{W_{eq}^H}\right)}} \tag{3.18}$$

for ZF precoder the estimated received signal ŝ is given by:

$$\begin{aligned} \hat{\mathrm{s}} &= \frac{1}{\alpha_{\mathrm{ZF}}} \left(\mathrm{H}\alpha_{\mathrm{ZF}}\mathrm{W_{ZF}}\mathrm{s} + \mathrm{n}\right) \\ &= \mathrm{s} + \frac{1}{\alpha_{\mathrm{ZF}}}\mathrm{n} \end{aligned} \tag{3.19}$$

and MMSE precoder:

$$\begin{aligned} \hat{\mathrm{s}} &= \frac{1}{\alpha_{\mathrm{MMSE}}} \left(\mathrm{H}\alpha_{\mathrm{MMSE}}\mathrm{W_{MMSE}}\mathrm{s} + \mathrm{n}\right) \\ &= \mathrm{s} + \frac{1}{\alpha_{\mathrm{MMSE}}}\mathrm{n} \end{aligned} \tag{3.20}$$

with $\mathrm{W_{ZF}}$ and $\mathrm{W_{MMSE}}$ equal to $\mathrm{H^H}\left(\mathrm{HH^H}\right)^{-1}$ or H^{-1} and $\mathrm{H^H}\left(\mathrm{HH^H} + \sigma_{\mathrm{z}}^2\mathrm{I}\right)^{-1}$ respectively. Note that using the precoder at the transmitter side, outperforms the receiver-side, since the receiver-side equalization (spatial multiplexing linear detection) suffers from noise enhancement [14]. Y. S. Cho *et al.* [14] also analyses the performance of ZF and MMSE equalizers applied at transmitter and receiver presented in Figure 3.7.

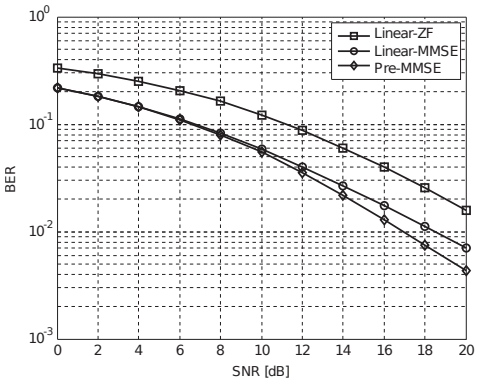

Figure 3.7: Performance comparison: receiver-side ZF/MMSE vs. pre-MMSE equalization (source [14])

CHAPTER 4

Field Programmable Gate Arrays (FPGAs)

This chapter presents a description of what is an Field Programmable Gate Array (FPGA) and how can they be programmed.

4.1 FPGA

Field Programmable Gate Arrays (FPGAs) are semiconductor hardware devices with the possibility of being programmed several times Static Random-Access Memory (SRAM)-based or One-Time Programmable (OTP) (impossibility to reprogram). FPGAs are constituted by matrix based Configurable Logic Blocks (CLBs) whose interconnections can be programable [25]. The reprogrammable ability allows hardware designers to improve the FPGA based designs at later developer stages of even after shipping. This possibility makes it possible to reuse the same resources often and reduce development costs.

FPGA basic blocks: CLBs (depict Figure 4.1) consists of a configurable switch matrix and some selective circuitry like multiplexers, and flip-flops. The number of available features at each CLBs may vary between devices but the switch matrix is flexible enough and can be configured to handle shift registers, combinatorial logic, Random-Access Memory (RAM), etc.

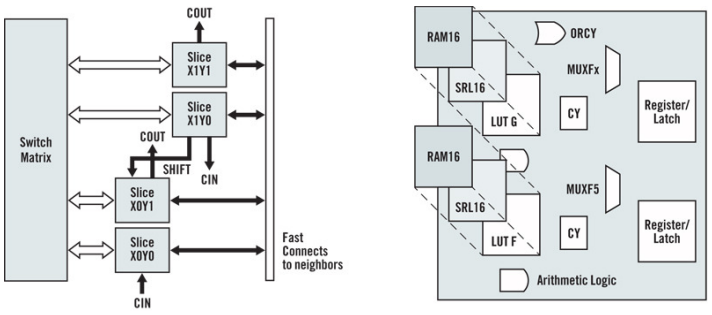

Figure 4.1: Basic Configurable Logic Blocks (CLBs) structure (source [25])

At Table 4.1 we can see the specifications of the commercial available FPGAs. Other vendors exist, being the common ones: Xilinx, Altera, Actel and Atmel [26]. In order to program the FPGA, the user must provide a Hardware Description Language (HDL) (examples of HDL languages are: VHDL and Verilog) or a schematic design. HDL is a better choice when working with large structures, since

Features	Artix™-7	Kintex™-7	Virtex® -7	Spartan® -6	Virtex-6
Logic Cells	215000	480000	2000000	150000	760000
BlockRAM	13Mb	34Mb	68Mb	4.8Mb	38Mb
DSP Slices	740	1920	3600	180	2016
DSP Performance (symmetric FIR)	930 GMACS	2,845 GMACS	5,335 GMACS	140 GMACS	2,419 GMACS
Transceiver Count	16	32	96	8	72
Transceiver Speed	6.6Gb/s	12.5Gb/s	28.05Gb/s	3.2Gb/s	11.18Gb/s
Total Transceiver Bandwidth (full duplex)	211Gb/s	800Gb/s	2,784Gb/s	50Gb/s	536Gb/s
Memory Interface (DDR3)	1,066Mb/s	1,866Mb/s	1,866Mb/s	800Mb/s	1,066Mb/s
PCI Express® Interface	x4 Gen2	Gen2x8	Gen3x8	Gen1x1	Gen2x8
Analog Mixed Signal (AMS)/XADC	Yes	Yes	Yes	-	Yes
Configuration AES	Yes	Yes	Yes	Yes	Yes
I/O Pins	500	500	1200	576	1200
I/O Voltage	1.2V, 1.35V, 1.5V, 1.8V, 2.5V, 3.3V	1.2V, 1.35V, 1.5V, 1.8V, 2.5V, 3.3V	1.2V, 1.35V, 1.5V, 1.8V, 2.5V, 3.3V	1.2V, 1.5V, 1.8V, 2.5V, 3.3V	1.2V, 1.5V, 1.8V, 2.5V
EasyPath™ Cost Reduction Solution	-	Yes	Yes	-	Yes

Table 4.1: Xilinx FPGA families (source: [25])

it's possible to just specify the options and intercommunications numerically instead of drawing each one by hand. However a schematic makes easier to the user to visualize and interpret a design. The next step is to generate the technology-mapped netlist, that can be performed using an Electronic Design Automation (EDA) tool. That netlist needs then to be fitted in a specific FPGA architecture, a place-and-route software will then try to fit and optimize the netlist. The final process passes through the generation of a binary file and transfer it to the FPGA via a serial interface (JTAG) or external memory device like an Electrically-Erasable Programmable Read-Only Memory (EEPROM) [27].

4.2 SYSTEM GENERATOR

System Generator is a XILINX® toolbox with Simulink® (a MATLAB® simulation enviroment) integration. System Generator makes possible to implement and simulate FPGA based circuitry, using a Graphical User Interface (GUI), with a set of pre-developed XILINX® blocks. The blocks can be interconnected with wires, representing each one a signal flows or a bus of signals/data.

Simulink integration makes possible to: generate test vectors with Matlab or Simulink blocks, better data visualization, design analysing and analogue/discrete simulations. The interface between System Generator and Symulink block, have to be made using a special type of blocks: Gateway In and Gateway out that handles the double to fixed point conversions, and vice versa shown in Figure 4.2. In between these interface blocks are the Xilinx blocks, the only ones which will be synthesized. There is also a special block called "System Generator Token", this block is mandatory in every System Generator project, and within are the simulation and hardware parameters (eg: sample period, hardware clock, target FPGA model, etc.)

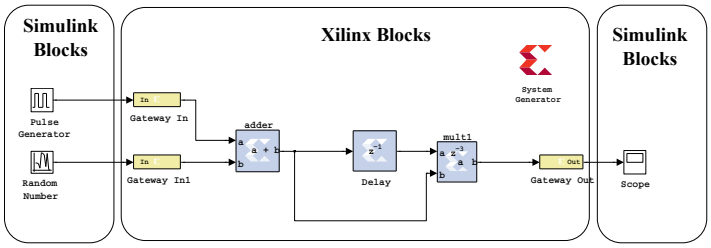

Figure 4.2: Interface between System Generator and Simulink blockset

Besides the special blocks, many other blocks are also available, depicted in Figure 4.3 at the Xilinx blockset, and are divided in the following categories: AXI4, Basic Elements, Communication, Control Logic, DSP, Data Types, Floating-Point, Index, Math, Memory and Tools.

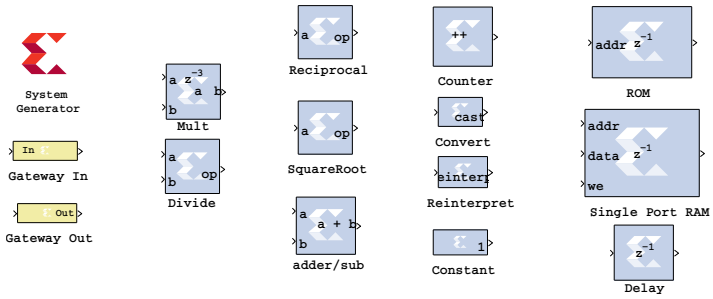

Figure 4.3: Example of System Generator blocks

CHAPTER 5

Implementation and Results

This chapter presents the proposed system for SM-MIMO precoder, a Matlab simulator, description the FPGA implementation and test of some blocks using System Generator.

5.1 PROPOSED SYSTEM

In order to implement a Spatial Multiplexing MIMO (SM-MIMO) precoder in hardware (FPGA), and after reviewing the literature we opted for the implementation of the following system: see Figure 5.1, with the preoccupation of developing a system that is modular enough to be possible and easy add or change features as well as improvements.

The proposed system modulates data streams, applies the precoder (precoder matrix is estimated with the channel information relayed from the receiver) to them with power constraints and sends them through the H channel. At the receiver the channel is estimated, relayed back to the transmitter; power correction is applied and symbols are demodulated (see Figure 5.1).

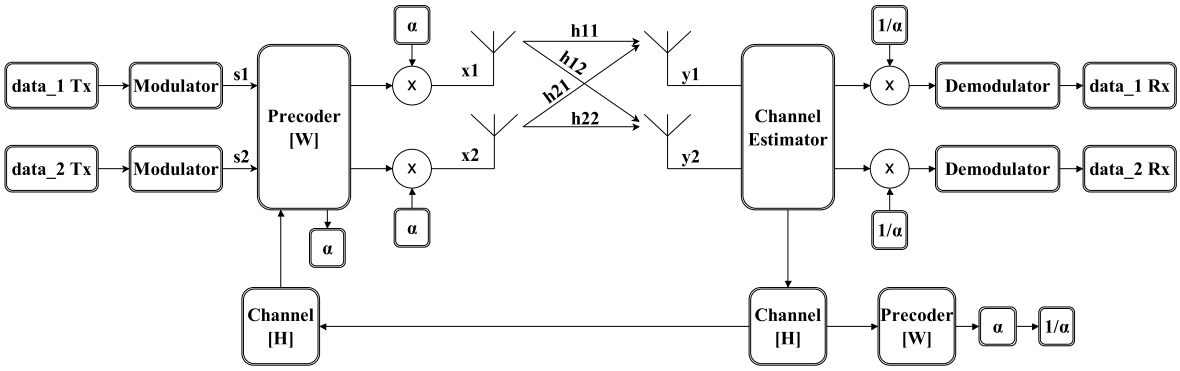

Figure 5.1: Proposed system diagram – frequency implementation

In order to perform the power constraint correction at the receiver, α coefficients are needed at the receiver. Those could be transmitted from the transmitter to the receiver, since they are estimated at the transmitter. But since SM-MIMO is a multiplexing technique whose purpose is to increase bandwidth, we tried not to reduce the effective data-rate by estimating it again at the receiver.

5.2 SM-MIMO MATLAB® SIMULATION

A Matlab based SM-MIMO precoder simulator (Matlab code is available at Appendix A) was implemented based on the proposed system presented on the Figure 5.1 at Section 5.1.

As depicted in Figure 5.2 the SM-MIMO implementation using a ZF precoder have a worse BER in comparison to the MMSE precoder. This result is expected accordingly to the theoretical predictions described in Section 3.2.2, effectively exits a gain difference of 3 dB for the same BER. The data was obtained using QPSK modulation, 100000 OFDM symbols with 768 sub-carriers each and varying the SNR from 0 to 20 dB and using an AWGN channel.

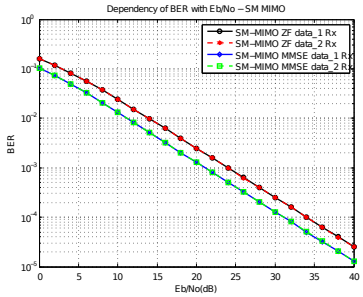

Figure 5.2: SM-MIMO BER for ZF and MMSE precoders

Let's analyse some signals of the Matlab implementation of the SM-MIMO precoder[1]. At Figure 5.3a it is shown the complex values of the channel matrix inversion for ZF precoder, note the high amplitude of some values ($\|W_{i,j}\|$), demonstrating the necessity for the usage of power constraint. Depicting Figure 5.3b we observe the effect of the usage of the power normalization.

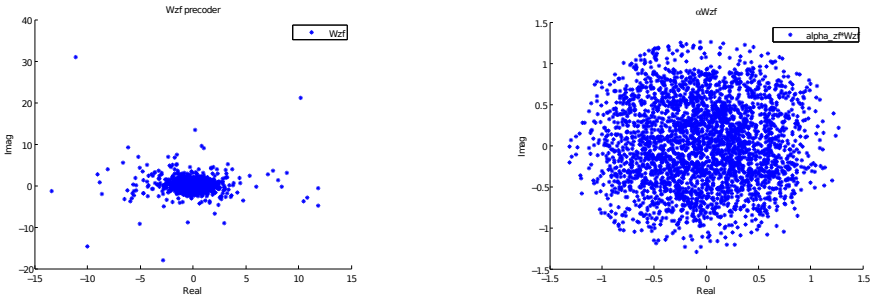

(a) (b)

Figure 5.3: Eb/N_0=8: (a) Wzf (b) alpha_zf*Wzf

At the receiver, the received signal Yzf shown in Figure 5.4a is affected by the noise and due to the power constraint, the magnitude of the QPSK symbols was affected. To solve this issue, multiplication by 1/alpha_zf is performed having finally the $\hat{s}$ signal, the result is shown in Figure 5.4b.

[1]Each graph has 768 points, one point of each sub-carrier in a OFDM symbol

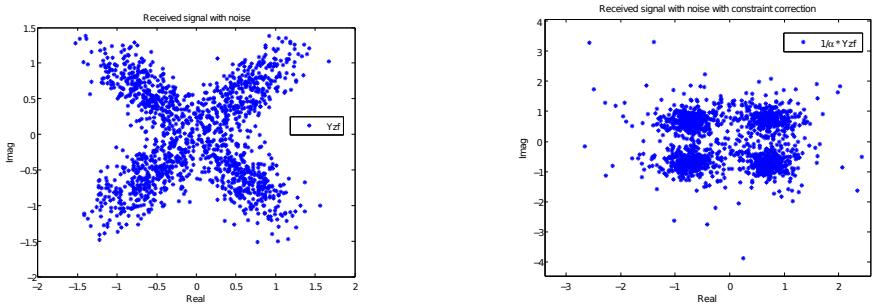

(a) (b)

Figure 5.4: Eb/N_0=8: (a) Yzf (b) 1/alpha_zf*Yzf

If we increase the SNR the QPSK constellation approximates to a ideal one. Similar results are obtained for the MMSE precoder, the difference is that it achieves better BER with the same SNR.

5.3 SYSTEM GENERATOR IMPLEMENTATION

Implementing a SM-MIMO precoder in a FPGA is a lot more challenging than implementing in Matlab, even if we use a GUI for schematic design like System Generator. The main drawbacks are:

- System Generator mathematical operations are very limited, only basic operations, are provided.
- Complex operations' blocks are even more limited.
- Recommended usage of Fixed point in FPGAs in order to space some space.
- Timings, data propagation factors, etc.

Before showing the individual blocks, lets present the final block shown in Figure 5.5 and it's interfaces. Accordingly to the proposed system the precoder block also inputs the modulated data symbols s and returns the x_i signals already with power constraint. There are some extra inputs and outputs ports, specific for fpga implementation: enable, addr, and data valid ports.

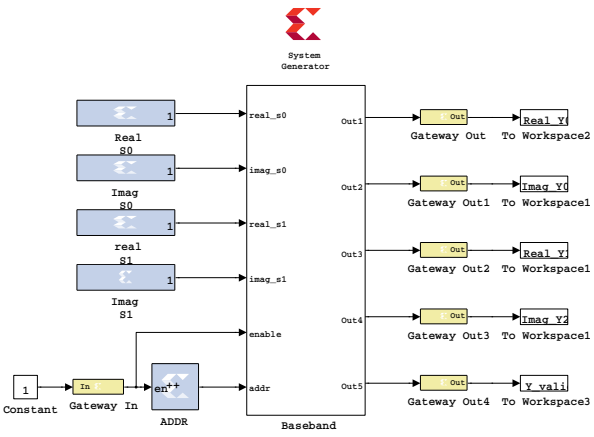

Figure 5.5: SM-MIMO implementation: main block

Inside Baseband block on main block, several operations need to be performed, namely: H matrix inversion, $W = H^{-1}$, alpha_zf calculation, multiply alpha_zf to W (power constraint) and finally matrix multiplication of symbols with W depict Figure 5.6

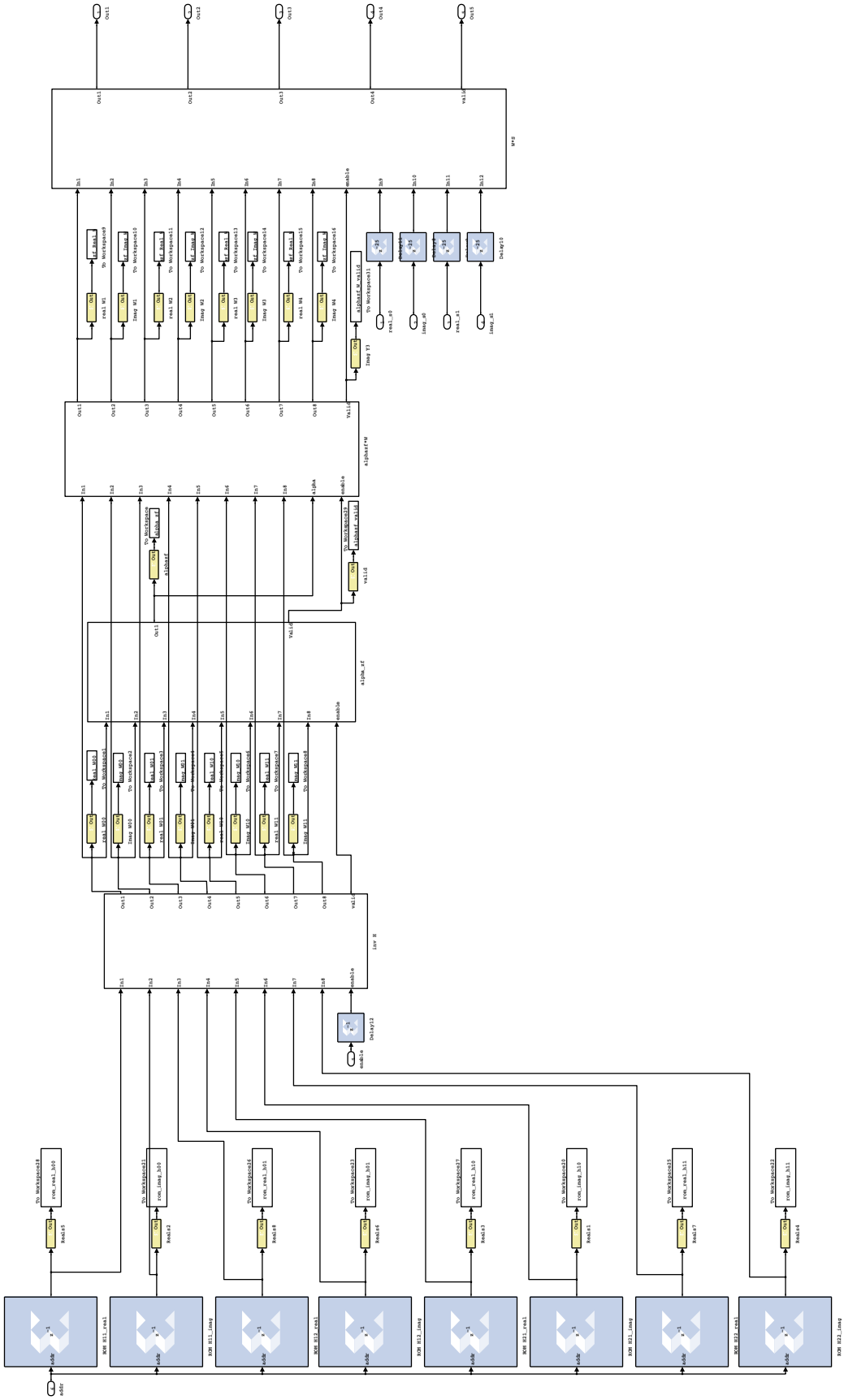

Figure 5.6: SM-MIMO implementation: [baseband] block

Channel inversion is performed using the Cramer's rule:

$$\begin{bmatrix} \mathrm{H}_{00} & \mathrm{H}_{01} \\ \mathrm{H}_{10} & \mathrm{H}_{11} \end{bmatrix}^{-1} = \frac{1}{\det(\mathrm{H})} \begin{bmatrix} \mathrm{H}_{11} & -\mathrm{H}_{01} \\ -\mathrm{H}_{10} & \mathrm{H}_{00} \end{bmatrix} = \frac{1}{\mathrm{H}_{00}\mathrm{H}_{11} - \mathrm{H}_{01}\mathrm{H}_{10}} \begin{bmatrix} \mathrm{H}_{11} & -\mathrm{H}_{01} \\ -\mathrm{H}_{10} & \mathrm{H}_{00} \end{bmatrix} \tag{5.1}$$

assuming $\mathrm{H}_{00}\mathrm{H}_{11} - \mathrm{H}_{01}\mathrm{H}_{10} = \alpha + j\beta$ then H^{-1} equals:

$$\begin{bmatrix} \frac{\mathrm{h}_{11\mathrm{r}}+j\mathrm{h}_{11\mathrm{i}}}{\alpha+j\beta} & \frac{-\mathrm{h}_{01\mathrm{r}}-j\mathrm{h}_{01\mathrm{i}}}{\alpha+j\beta} \\ \frac{-\mathrm{h}_{10\mathrm{r}}-j\mathrm{h}_{10\mathrm{i}}}{\alpha+j\beta} & \frac{\mathrm{h}_{00\mathrm{r}}+j\mathrm{h}_{00\mathrm{i}}}{\alpha+j\beta} \end{bmatrix} \tag{5.2}$$

complex expanding the equations, becomes:

$$\begin{bmatrix} \mathrm{H}_{00} & \mathrm{H}_{01} \\ \mathrm{H}_{10} & \mathrm{H}_{11} \end{bmatrix}^{-1} = \begin{bmatrix} \frac{\mathrm{h}_{11\mathrm{r}}\alpha+\mathrm{h}_{11\mathrm{i}}\beta}{\alpha^2+\beta^2} + j\frac{\mathrm{h}_{11\mathrm{i}}\alpha-\mathrm{h}_{11\mathrm{r}}\beta}{\alpha^2+\beta^2} & \frac{-\mathrm{h}_{01\mathrm{r}}\alpha-\mathrm{h}_{01\mathrm{i}}\beta}{\alpha^2+\beta^2} + j\frac{-\mathrm{h}_{01\mathrm{i}}\alpha+\mathrm{h}_{01\mathrm{i}}\beta}{\alpha^2+\beta^2} \\ \frac{-\mathrm{h}_{10\mathrm{r}}\alpha-\mathrm{h}_{10\mathrm{i}}\beta}{\alpha^2+\beta^2} + j\frac{-\mathrm{h}_{10\mathrm{i}}\alpha+\mathrm{h}_{10\mathrm{r}}\beta}{\alpha^2+\beta^2} & \frac{\mathrm{h}_{00\mathrm{r}}\alpha+\mathrm{h}_{00\mathrm{i}}\beta}{\alpha^2+\beta^2} + j\frac{\mathrm{h}_{00\mathrm{i}}\alpha-\mathrm{h}_{00\mathrm{r}}\beta}{\alpha^2+\beta^2} \end{bmatrix} \tag{5.3}$$

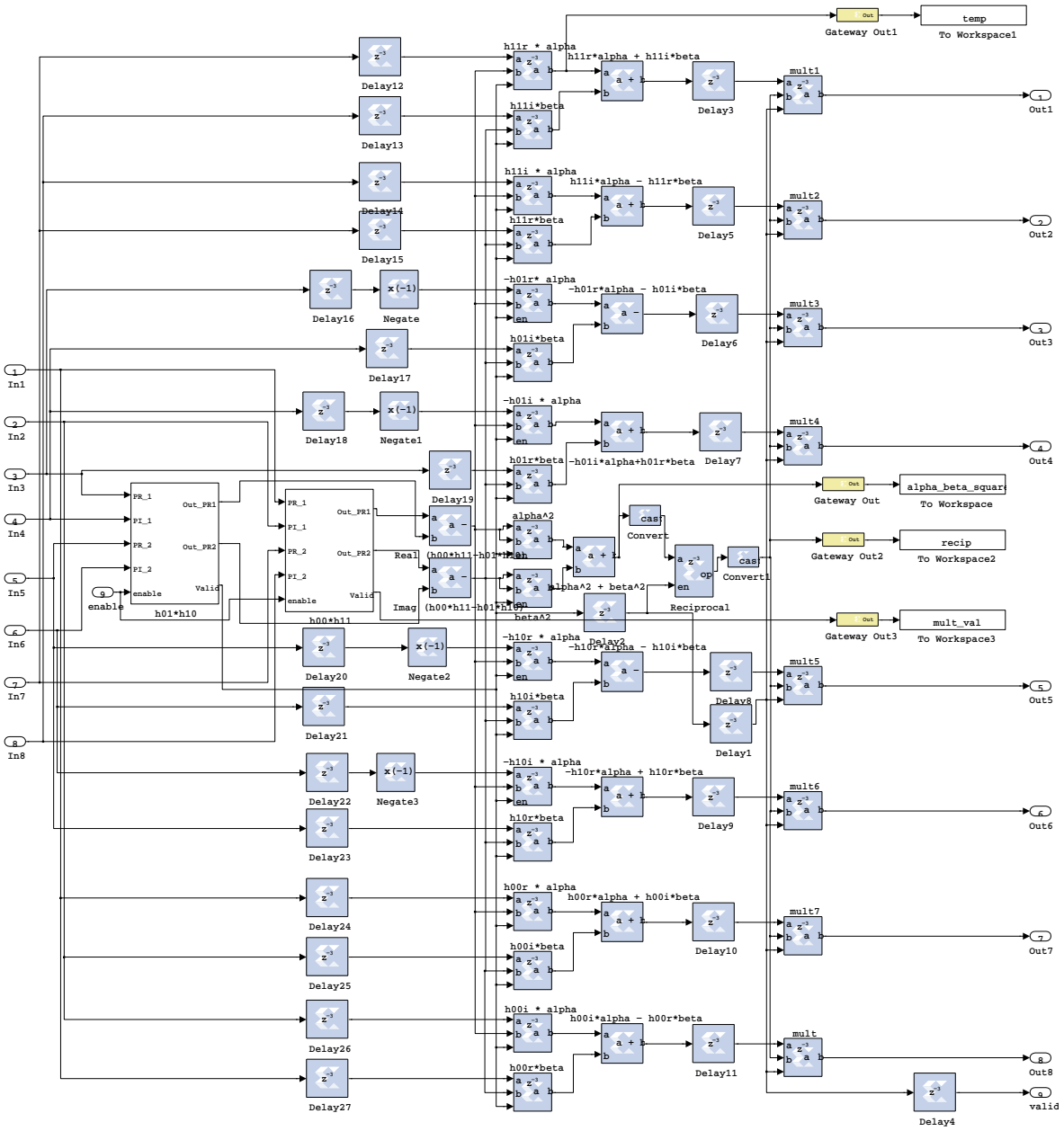

Figure 5.7: SM-MIMO implementation: [inv H] block

The following two blocks: h00*h11 and h01*h10 are complex multipliers implemented using regular multiplication blocks depict Figure 5.8.

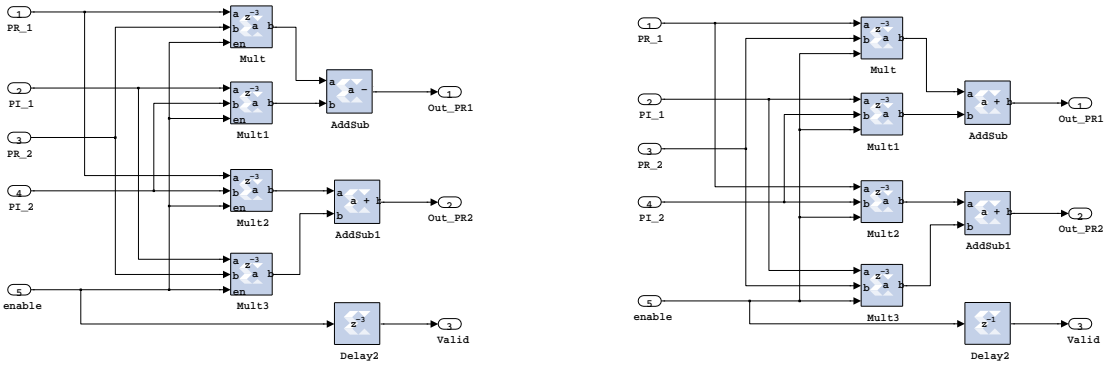

(a) (b)

Figure 5.8: SM-MIMO implementation: (a) [h00*h11] block (b) [h01*h10] block

In order to apply the power constraint, the constant α_{zf} needs to be estimated as follows:

$$\alpha_{\mathrm{zf}} = \sqrt{\frac{k}{\mathrm{Trace}\left(\mathrm{WW^H}\right)}} \tag{5.4}$$

with Trace being the sum of diagonal elements and $\mathrm{WW^H}$ equals:

$$\mathrm{WW^H} = \begin{bmatrix} \mathrm{W_{00}} & \mathrm{W_{01}} \\ \mathrm{W_{10}} & \mathrm{W_{11}} \end{bmatrix} \begin{bmatrix} \mathrm{W_{00}^H} & \mathrm{W_{10}^H} \\ \mathrm{W_{01}^H} & \mathrm{W_{11}^H} \end{bmatrix} \tag{5.5}$$

multiplying the two matrix becomes:

$$\mathrm{WW^H} = \begin{bmatrix} \mathrm{W_{00}W_{00}^H + W_{01}W_{01}^H} & \mathrm{X} \\ \mathrm{X} & \mathrm{W_{10}W_{10}^H + W_{11}W_{11}^H} \end{bmatrix} \tag{5.6}$$

expanding the multiplications become:

$$\mathrm{WW^H} = \begin{bmatrix} \mathrm{W_{00r}^2 + W_{00i}^2 + W_{01r}^2 + W_{01i}^2} & \mathrm{X} \\ \mathrm{X} & \mathrm{W_{10r}^2 + W_{10i}^2 + W_{11r}^2 + W_{11i}^2} \end{bmatrix} \tag{5.7}$$

Then α_{zf} finally becomes (implementation in Figure 5.9):

$$\alpha_{\mathrm{zf}} = \sqrt{\frac{k}{\mathrm{W_{00r}^2 + W_{00i}^2 + W_{01r}^2 + W_{01i}^2 + W_{10r}^2 + W_{10i}^2 + W_{11r}^2 + W_{11i}^2}} \tag{5.8}$$

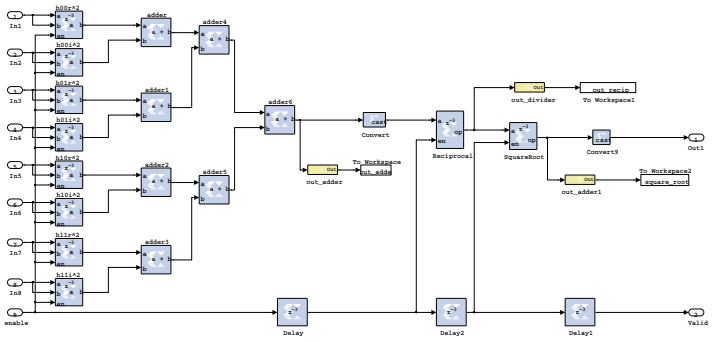

Figure 5.9: SM-MIMO implementation: [alpha_zf] block

The next block see Figure 5.10 performs a element-wise multiplication alphazf and W.

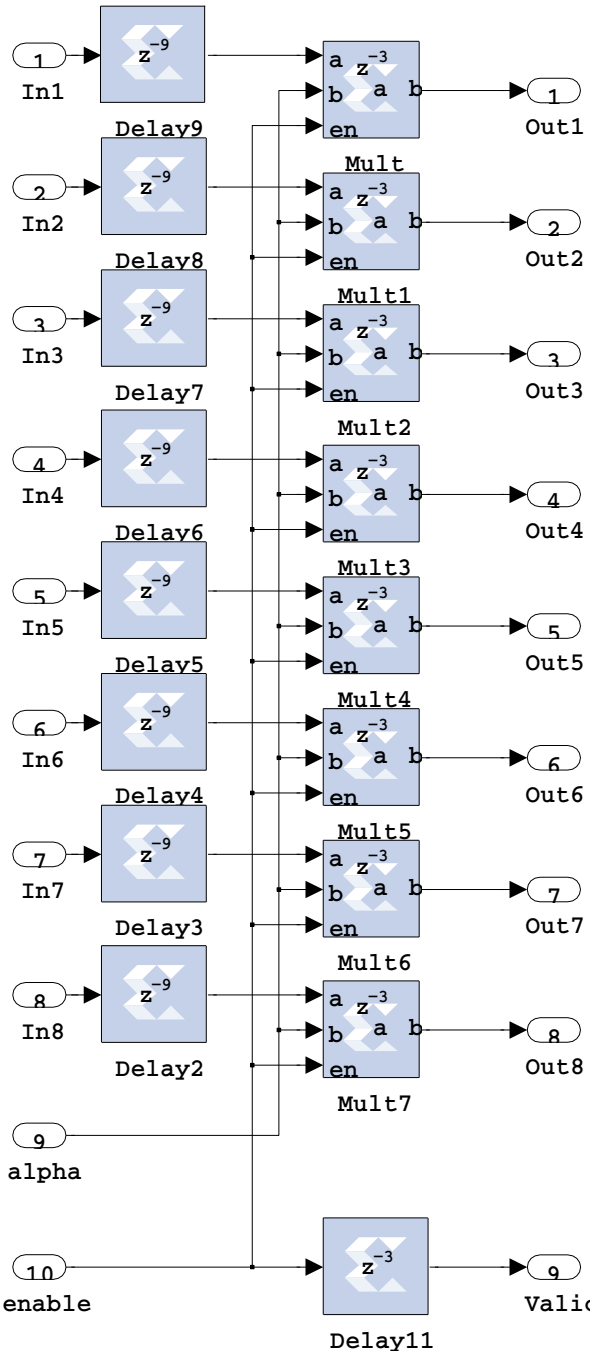

Figure 5.10: SM-MIMO implementation: [alphazf*W] block

W*S block performs the multiplication between matrix W and the s vector (W × s) as follows:

$$\mathrm{Ws} = \begin{bmatrix} \mathrm{W}_{00} & \mathrm{W}_{01} \\ \mathrm{W}_{10} & \mathrm{W}_{11} \end{bmatrix} \begin{bmatrix} \mathrm{s}_0 \\ \mathrm{s}_1 \end{bmatrix} \tag{5.9}$$

The implementation of this operation is shown in Figure 5.11.

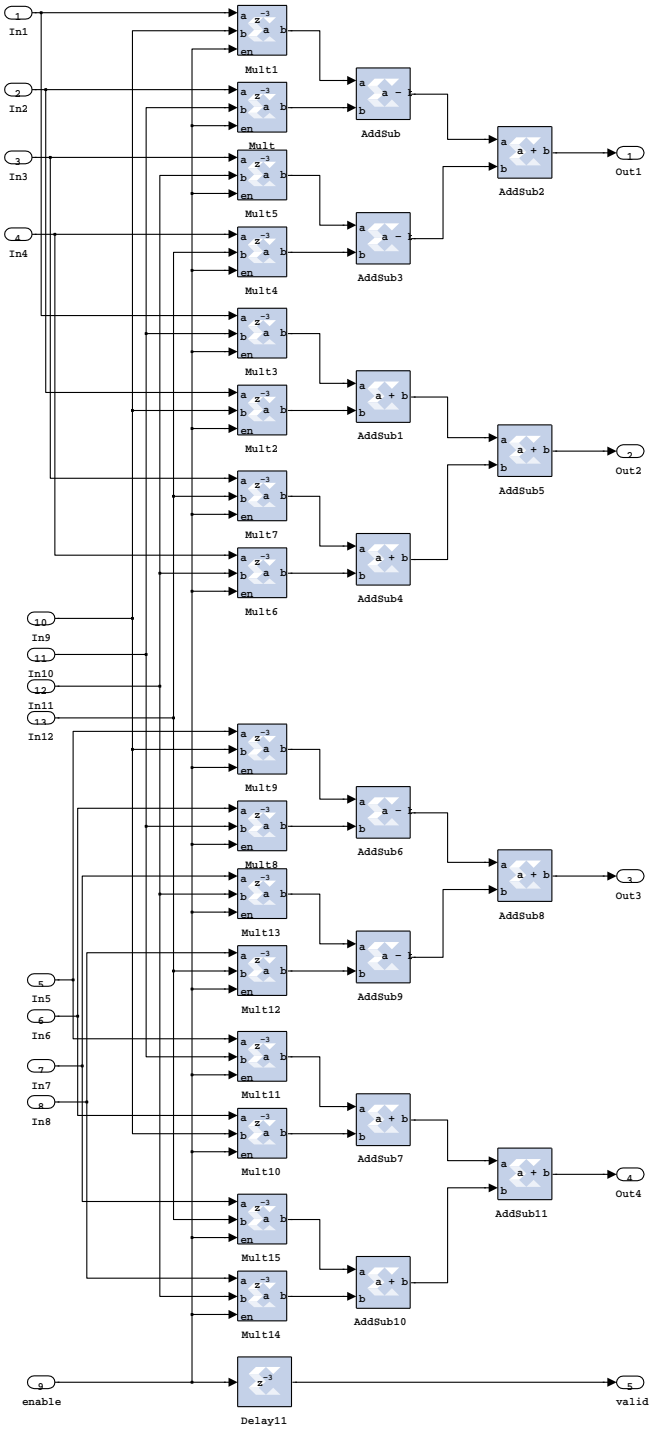

Figure 5.11: SM-MIMO implementation: [W*S] block

At Figure 5.12a we show a comparison between Matlab channel inversion (double precision) and inversion realized with System Generator blocks (fixed point precision). At figure 5.12b the comparison is realized between the two implementations but for channel inversion with power constraints.

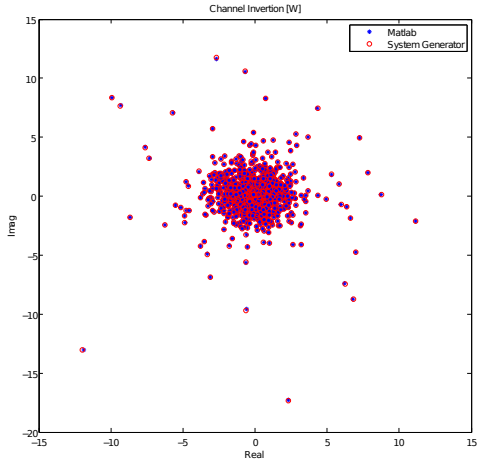

(a)

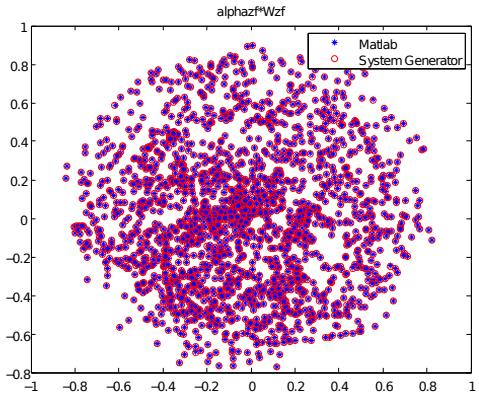

(b)

Figure 5.12: SM-MIMO precoder comparison between MATLAB® and System Generator implementations: (a) Channel Invertion $[W] = [H]^{-1}$ (b) $alpha\_zf[W]$

CHAPTER 6

Conclusion and Future Work

This chapter presents the final conclusions and some possibilities of future work.

6.1 CONCLUSION

The proposed system was implemented in Matlab, tested and validated. As expected using a ZF equalizer to precode, comparatively to MMSE, the BER was worse, we found a difference of -3dB for the same BER. A ZF precoder was implemented in System Generator, the baseband was tested and validated up to the power constraint block (transmission block).

6.2 FUTURE WORK

It would be useful to implement the uplink channel in order to send the channel information estimated in the MS to the BS. As the full FPGA integration wasn't realized, it would be useful to finish and test the SM-MIMO precoder in a real scenario in order to analyse its performance and practicality.

Regarding the precoder, it would be desirable to implement in System Generator/FPGA a MMSE precoder, in order to get better BER but it requires the variance of noise (estimated theoretically and experimentally confirmed).

APPENDIX A

SM-MIMO MATLAB® SIMULATOR

```
close all
clear all
clc
% Parameters
m=4; % 2:BPSK - 4:QPSK - 16:QAM-16
N_OFDM=100000;
N_SCARRIER=768;
N_bits=log2(m)*N_SCARRIER;
FFT_SIZE=1024;
FS=15.36E6;
CP=5.21E-6;
EBN0=0:2:20;
PR=1;
TS=1/FS;
NCP=round(CP/TS);
N_elem_tx=FFT_SIZE+NCP;
load('pdp.mat');            % load multipath elements

error_rate_zf_user1=zeros(1,N_OFDM);        % error rate
error_rate_zf_user2=zeros(1,N_OFDM);        % error rate
error_rate_mmse_user1=zeros(1,N_OFDM);      % error rate
error_rate_mmse_user2=zeros(1,N_OFDM);      % error rate
ber_zf_user1=zeros(1,length(EBN0));         % bit error rate
ber_zf_user2=zeros(1,length(EBN0));         % bit error rate
ber_mmse_user1=zeros(1,length(EBN0));       % bit error rate
ber_mmse_user2=zeros(1,length(EBN0));       % bit error rate

sigma2=zeros(1,length(EBN0));               % sigma squared
framing=zeros(1,FFT_SIZE);
size_zeros_framing=(FFT_SIZE-N_SCARRIER)/2;
Yzf=zeros(2,N_SCARRIER);
Ymmse=zeros(2,N_SCARRIER);
n=zeros(1,2);
noise=zeros(2,N_SCARRIER);
S=zeros(2,N_SCARRIER);
Si=zeros(2,1);
```

```
H=zeros(2,2);
Wzf=zeros(2,2);
Wmmse=zeros(2,2);
Hf11=zeros(1,N_SCARRIER);
Hf12=zeros(1,N_SCARRIER);
Hf21=zeros(1,N_SCARRIER);
Hf22=zeros(1,N_SCARRIER);
data_symbol_user1=zeros(1,N_SCARRIER);
data_symbol_user2=zeros(1,N_SCARRIER);
tx_user1=zeros(1,N_bits);
tx_user2=zeros(1,N_bits);
rx_zf_user1=zeros(1,N_bits);
rx_zf_user2=zeros(1,N_bits);
rx_mmse_user1=zeros(1,N_bits);
rx_mmse_user2=zeros(1,N_bits);
k=2;
Ik=eye(2);
% using toolbox
% h1=modem.qammod(m);
% h1.inputtype='bit';
% h1.symbolorder='gray';
% h2=modem.qamdemod(m);
% h2.outputtype='bit';
% h2.symbolorder='gray';
% h2.decisiontype='hard decision';


for p=1:length(EBN0)
    sigma2(p)=(PR.*10.^(-EBN0(p)/10))/log2(m);
    sigmasquared=sigma2(p);
    for l=1:N_OFDM

        % Data Genenerator
        tx_user1=data_gen(N_bits);
        tx_user2=data_gen(N_bits);

        % Modulation
        % data_symbol_user1=modulate(h1,tx_user1);
        % data_symbol_user2=modulate(h1,tx_user2);
        data_symbol_user1=mod_data(tx_user1, m); % m=1 BPFSK m=2; QPSK m=4; QAM-64 m
            =16
        data_symbol_user2=mod_data(tx_user2, m); % m=1 BPFSK m=2; QPSK m=4; QAM-64 m
            =16

        %S=[data_symbol_user1';data_symbol_user2'];
        S=[data_symbol_user1;data_symbol_user2];

        % H11
        [~,Hf11]=channel_gen(pdp,FS,N_SCARRIER); %FFT_SIZE
        %Hf11=Hf11(size_zeros_framing:N_SCARRIER+size_zeros_framing-1);

        % H21
        [~,Hf21]=channel_gen(pdp,FS,N_SCARRIER); %FFT_SIZE
        %Hf21=Hf21(size_zeros_framing:N_SCARRIER+size_zeros_framing-1);

        % H12
```

```
91          [~,Hf12]=channel_gen(pdp,FS,N_SCARRIER); %FFT_SIZE
92          %Hf12=Hf12(size_zeros_framing:N_SCARRIER+size_zeros_framing-1);
93
94          % H22
95          [~,Hf22]=channel_gen(pdp,FS,N_SCARRIER); %FFT_SIZE
96          %Hf22=Hf22(size_zeros_framing:N_SCARRIER+size_zeros_framing-1);
97
98          % noise generator AWGN
99          noise=sqrt((sigma2(p)/2)).*[randn(1,N_SCARRIER)+1i*randn(1,N_SCARRIER);randn
                (1,N_SCARRIER)+1i*randn(1,N_SCARRIER)];
100         %noise=[zeros(1,N_SCARRIER);zeros(1,N_SCARRIER)];
101
102         for q=1:N_SCARRIER
103             % Grab 2 symbols [2x1]
104             Si=S(1:2,q);
105
106             % channel [2x2]
107             H=[Hf11(q),Hf21(q);Hf12(q),Hf22(q)];
108
109             % ZF: Zero forcing
110             % Replace inv(A)*b with A\b
111             % Replace b*inv(A) with b/A
112             % Note: MATLAB computes X^(-1) and inv(X) in the same manner,
113             % and both are subject to the same limitations.
114             Wzf=H'/(H*H');
115
116             alphazf=sqrt(k/trace(Wzf*Wzf'));
117             Wzf=alphazf*Wzf;
118
119             % Mininum Mean Square Error
120             Wmmse=H'/(H*H'+Ik*sigmasquared);
121
122             alphammse=sqrt(k/trace(Wmmse*Wmmse'));
123             Wmmse=alphammse*Wmmse;
124             % noise generator [2x1]
125             n=noise(1:2,q);
126
127             % Antenna 1 and Antenna 2: RX Signal [Yzf]
128             Yzf(1:2,q)=(1/alphazf)*(H*(Wzf*Si)+n);
129
130             % Antenna 1 and Antenna 2: RX Signal [Ymmse]
131             Ymmse(1:2,q)=(1/alphammse)*(H*(Wmmse*Si)+n);
132         end
133
134         % rx_zf_user1=demodulate(h2,Yzf(1,:)');
135         % rx_zf_user2=demodulate(h2,Yzf(2,:)');
136
137         rx_zf_user1=demod_data(Yzf(1,:),m,N_bits);
138         rx_zf_user2=demod_data(Yzf(2,:),m,N_bits);
139
140         % rx_mmse_user1=demodulate(h2,Ymmse(1,:)');
141         % rx_mmse_user2=demodulate(h2,Ymmse(2,:)');
142
143         rx_mmse_user1=demod_data(Ymmse(1,:),m,N_bits);
144         rx_mmse_user2=demod_data(Ymmse(2,:),m,N_bits);
145
```

```
        error_rate_zf_user1(l)=sum(rx_zf_user1 ~= tx_user1)/N_bits;
        error_rate_zf_user2(l)=sum(rx_zf_user2 ~= tx_user2)/N_bits;
        error_rate_mmse_user1(l)=sum(rx_mmse_user1 ~= tx_user1)/N_bits;
        error_rate_mmse_user2(l)=sum(rx_mmse_user2 ~= tx_user2)/N_bits;
    end
    ber_zf_user1(p)=mean(error_rate_zf_user1);
    ber_zf_user2(p)=mean(error_rate_zf_user2);
    ber_mmse_user1(p)=mean(error_rate_mmse_user1);
    ber_mmse_user2(p)=mean(error_rate_mmse_user2);
    fprintf('%.2f%% Complete\n',(p/length(EBN0))*100);
end

savefile = 'sm_mimo_frequency.mat';
save(savefile,'EBN0','N_OFDM','ber_zf_user1','ber_zf_user2','ber_mmse_user1','
    ber_mmse_user2');

figure()
load('sm_mimo_frequency.mat');
semilogy(EBN0,ber_zf_user1,'o-','LineWidth',1.5,'MarkerSize',5);
hold on
grid on
semilogy(EBN0,ber_zf_user2,'hk-','LineWidth',1.5,'MarkerSize',5);
semilogy(EBN0,ber_mmse_user1,'rd--','LineWidth',1.5,'MarkerSize',5);
semilogy(EBN0,ber_mmse_user2,'gs--','LineWidth',1.5,'MarkerSize',5);

title('Dependency of BER with Eb/No - SM MIMO')
xlabel('Eb/No(dB)');
ylabel('BER');
legend('SM-MIMO ZF User1 [2x2]','SM-MIMO ZF User 2 [2x2]','SM-MIMO MMSE User 1 [2x2]',
    'SM-MIMO MMSE User 2 [2x2]');

function data_symbol=mod_data(data, m)
% Data Modulation
%BPSK, m=2
%QPSK, m=4,
%16-QAM, m=16

switch m
    case 2
        data_symbol = -data*2+1; %mapping of 1->-1 and 0->1

    case 4
        % Coding of data bits in QPSK symbols - using Grey coding
        % (00->1+i; 01->1-i; 10->-1+i; 11->-1-i)
        % bit MS defines real polarity
        % bit LS defines imag polarity
        data_temp = reshape(data,2,length(data)/2);
        data_real = data_temp(1,:);
        data_imag = data_temp(2,:);
        data_symbol = sqrt(2)/2*((-1).^(data_real)+i*(-1).^(data_imag));

     case 16
        data_temp = reshape(data,4,length(data)/4);
        data_r1 = data_temp(1,:);
        data_i1 = data_temp(2,:);
        data_r2 = data_temp(3,:);
```

```
        data_i2 = data_temp(4,:);
        data_symbol = 2/sqrt(10).*(0.5*(-1).^(data_r2).*(-1).^(data_r1)+(-1).^(
            data_r1)+i.*(0.5*(-1).^(data_i2).*(-1).^(data_i1)+ (-1).^(data_i1)));
      otherwise
        helpdlg('Constellation size (m) not available');

end

function decoded_data=demod_data(data_symbol, m, N_Data)
vect_IMAG = imag(data_symbol);
vect_REAL = real(data_symbol);
coder_type_value=0;
switch m
    case 2
        if (coder_type_value==0)
                %hard decision
              decoded_data= ceil(-vect_REAL./(1.0000000000001.*max(abs(vect_REAL))));

        else
                %soft decision
                decoded_data = vect_REAL;
        end

    case 4
        % Decoding of data bits in QPSK symbols - using Grey coding
        % (1+i->00; 1-i->01; -1+i->10; -1-i->11)
        % real polarity defines bit MS
        % imag polarity defines bit LS
        if (coder_type_value==0)
                %hard decision
                vect_REAL_1 = ceil(-vect_REAL./(1.0000000000001.*max(abs(vect_REAL))))
                    ;
                vect_IMAG_1 = ceil(-vect_IMAG./(1.0000000000001.*max(abs(vect_IMAG))))
                    ;
                decoded_data = reshape([vect_REAL_1; vect_IMAG_1],1,N_Data);
        else
                %soft decision
                decoded_data = reshape([vect_REAL; vect_IMAG],1,N_Data);
        end
    case 16
        P_1= vect_REAL;
        P_2= vect_IMAG;
        P_3= abs(vect_REAL)-2/sqrt(10);
        P_4= abs(vect_IMAG)-2/sqrt(10);
        if (coder_type_value==0)
            %hard decision
            vect_IMAG_1 = ceil(-P_2./(1.0000000000001.*max(abs(P_2))));
            vect_IMAG_2 = ceil(-P_4./(1.0000000000001.*max(abs(P_4))));
            vect_REAL_1 = ceil(-P_1./(1.0000000000001.*max(abs(P_1))));
            vect_REAL_2 = ceil(-P_3./(1.0000000000001.*max(abs(P_3))));
            decoded_data =  reshape([vect_REAL_1; vect_IMAG_1; vect_REAL_2;
                vect_IMAG_2],1,N_Data);
        else
            %soft decision
            decoded_data =  reshape([P_1; P_2; P_3; P_4],1,N_Data);
        end
```

```
252
253     otherwise
254         helpdlg('Constellation size (m) not available');
255 end
256
257 function y=data_gen(N_bits)
258     y=randi(2,1,N_bits)-1;
259 end
260
261 function y=conv_s_h(s,h,pdp,Nc,samp_freq,tg)
262 %tg=5.21e-6;                        % guerad time -> 80 samples
263
264 delays=pdp(:,1);
265 delta_t=1/samp_freq;
266 Npaths = length(delays);          % No. of paths considered for the channel
267 deltans=delta_t/1e-9;             % Sampling interval in ns
268 delays = round(delays/(deltans))+1;
269 Ng= round(tg/(delta_t))+1;
270 f_zeros=find(h==0);
271 h(f_zeros)=[];
272
273 aux = zeros(Npaths,Nc+Ng);
274
275 for n=1:Npaths
276     conv_sh=h(n)*s;
277     aux(n,delays(n):Nc+Ng-1+delays(n)-1)=conv_sh;
278 end
279
280 y=sum(aux);
281 y=y(1:Nc+Ng-1);
282
283 function [ht, Hf]=channel_gen(pdp,samp_freq, Nc)
284
285 delta_t=1/samp_freq;              %sample duratiion
286 Npaths = length(pdp(:,1));        % No. of paths considered for the channel
287 deltans=delta_t/1e-9;             % Sampling interval in ns
288
289 path_pot_lin=10.^(pdp(:,2)/10);
290 path_pot_lin=path_pot_lin./sum(path_pot_lin);
291
292 delays = pdp(:,1);
293 delays = round(delays./(deltans))+1;
294
295 multipath = zeros(1,Npaths);
296
297 for n=1:Npaths
298     pot_componente=0.5;
299     multipath(n)=sqrt(pot_componente)*randn(1,1)+1i*sqrt(pot_componente)*randn(1,1);
300     multipath(n)=multipath(n).*sqrt(path_pot_lin(n));
301 end
302
303 RI=zeros(1,Nc);
304 RI(delays) = RI(delays) + multipath;
305
306 ht=RI;
307 Hf=fft(ht);
```

References

[1] 3GPP, *About 3GPP*, Jun. 2014. [Online]. Available: http://www.3gpp.org/about-3gpp..

[2] E. Dahlman, S. Parkvall and J. Skold, *4G: LTE/LTE-Advanced for Mobile Broadband*. Elsevier Science, 2013, ISBN: 9780124199972.

[3] 3GPP, *3GPP organizational partners*, Jun. 2014. [Online]. Available: http://www.3gpp.org/about-3gpp/partners..

[4] A. Kumar, D. Y. Liu and J. Sengupta, «Evolution of mobile wireless communication networks: 1G to 4G», *International Journal of Electronics & Communication Technology, IJECT*, vol. 1, no. 1, 2010.

[5] ITU, *Global ICT developments*, Jul. 2014. [Online]. Available: http://www.itu.int/en/ITU-D/Statistics/Pages/stat/default.aspx..

[6] Y. G. Li and G. L. Stuber, *Orthogonal frequency division multiplexing for wireless communications*. Springer, 2006.

[7] T. S. Rappaort, *Wireless communications: principles and practice*. Prentice-Hall, 2002.

[8] Y. Okumura et al., «Field strength and its variability in vhf and uhf land-mobile radio service», *ELEC. COMM. LAB.*, vol. 16, 1968.

[9] M. Hata, «Empirical formula for propagation loss in land mobile radio services», *Vehicular Technology, IEEE Transactions on*, vol. 29, no. 3, pp. 317–325, Aug. 1980, ISSN: 0018-9545. DOI: 10.1109/T-VT.1980.23859.

[10] U. Godse, *Analog Communication*. Technical Publications, 2010, ISBN: 9788184311402. [Online]. Available: http://books.google.pt/books?id=6XH7BUqm-lIC.

[11] J. G. Proakis, *Digital communications*, 2001.

[12] S. Coleri, M. Ergen, A. Puri and A. Bahai, «Channel estimation techniques based on pilot arrangement in ofdm systems», *Broadcasting, IEEE Transactions on*, vol. 48, no. 3, pp. 223–229, 2002.

[13] S. Ohno, E. Manasseh and M. Nakamoto, «Preamble and pilot symbol design for channel estimation in ofdm systems with null subcarriers», *EURASIP Journal on Wireless Communications and Networking*, vol. 2011, no. 1, pp. 1–17, 2011.

[14] Y. S. Cho, J. Kim, W. Y. Yang and C. G. Kang, *MIMO-OFDM wireless communications with MATLAB*. John Wiley & Sons, 2010.

[15] K. Du and N. Swamy, *Wireless Communication Systems: From RF Subsystems to 4G Enabling Technologies*. Cambridge University Press, 2010, ISBN: 9781139485760. [Online]. Available: http://books.google.pt/books?id=5dGjKLawsTkC.

[16] D. Tse and P. Viswanath, *Fundamentals of wireless communication*. Cambridge university press, 2005.

[17] C. Oestges and B. Clerckx, *MIMO wireless communications: from real-world propagation to space-time code design*. Academic Press, 2010.

[18] A. Goldsmith, *Wireless communications*. Cambridge university press, 2005.

[19] M. K. Simon and M.-S. Alouini, *Digital communication over fading channels*. John Wiley & Sons, 2005, vol. 95.

[20] M. Jankiraman, *Space-time codes and MIMO systems*. Artech House, 2004.

[21] S. Alamouti, «A simple transmit diversity technique for wireless communications», *Selected Areas in Communications, IEEE Journal on*, vol. 16, no. 8, pp. 1451–1458, 1998.

[22] E. Dahlman, S. Parkvall, J. Skold and P. Beming, *3G evolution: HSPA and LTE for mobile broadband*. Academic press, 2010.

[23] G. Strang, *Linear Algebra and Its Applications 2nd Edition*. Academic Press, Inc., 1980.

[24] Y. Jiang, M. K. Varanasi and J. Li, «Performance analysis of zf and mmse equalizers for mimo systems: an in-depth study of the high snr regime», *Information Theory, IEEE Transactions on*, vol. 57, no. 4, pp. 2008–2026, 2011.

[25] Xilinx, *What is a fpga?*, Jul. 2014. [Online]. Available: `http://www.xilinx.com/fpga/index.htm`..

[26] R. Wiśniewski, *Synthesis of compositional microprogram control units for programmable devices*. University of Zielona Góra, 2009.

[27] Xilinx, *Implementation overview for fpgas*, Jul. 2014. [Online]. Available: `http://www.xilinx.com/support/documentation/sw_manuals/xilinx11/ise_c_implement_fpga_design.htm`..